OPEN ACCESS
Mathematics Open
Vol. 5 (2026) 2650020 (33 pages)
© The Author(s)
DOI: 10.1142/S2811007226500203

World Scientific
www.worldscientific.com

Math. Open 2026.05. Downloaded from www.worldscientific.com
by 196.43.164.50 on 11/12/26. Re-use and distribution is strictly not permitted, except for Open Access articles.

Optimal control analysis of transmission dynamics and treatment pathways in a TB–HCV co-infection model

Michael Byamukama* and Mohammed Kizito†

Department of Mathematics, Mbarara University of Science and Technology, P. O. Box 1410, Mbarara, Uganda
*mbyamukama@must.ac.ug
†kmohammed@must.ac.ug

Received 12 March 2026
Accepted 11 August 2026
Published 31 August 2026

This study develops a deterministic compartmental model to investigate the effects of partial treatment on the transmission dynamics of tuberculosis (TB) and hepatitis C virus (HCV) co-infection and to identify effective intervention strategies. The basic reproduction number was derived using the next-generation matrix method, and sensitivity analysis was conducted to determine the parameters most influential in disease transmission. The results show that transmission-related parameters have the greatest influence on the reproduction number, while treatment-related parameters substantially reduce the burden of TB–HCV co-infection. Numerical simulations further indicate that partial treatment prolongs infectiousness, accelerates disease progression, and enhances interactions between TB and HCV, with TB identified as the dominant contributor to co-infection dynamics. An optimal control model incorporating awareness, detection, and treatment interventions was formulated using Pontryagin's Maximum Principle. Numerical simulations demonstrate that the simultaneous implementation of these interventions can substantially reduce TB–HCV co-infection, with near elimination achievable within two years. Based on these findings, individuals diagnosed with either TB or HCV should be routinely screened for the other infection to facilitate early detection and timely concurrent treatment.

Keywords: Tuberculosis; hepatitis C; co-infection; deterministic model; partial treatment; optimal control.

1. Introduction

Tuberculosis (TB) remains a major global health challenge, as indicated by World Health Organization (WHO). Each year, it causes over 10 million new infections and

*Corresponding author.

This is an Open Access article published by World Scientific Publishing Company. It is distributed under the terms of the Creative Commons Attribution-NonCommercial 4.0 (CC BY-NC) License, which permits use, distribution and reproduction in any medium, provided that the original work is properly cited and is used for non-commercial purposes.

Math. Open 2026.05. Downloaded from www.worldscientific.com
by 196.43.164.50 on 11/12/26. Re-use and distribution is strictly not permitted, except for Open Access articles.

approximately 1.6 million deaths worldwide [61, 62]. In 2023, TB was once again the leading cause of mortality from a single infectious pathogen, with continued rise in cases since 2021 [61]. Although the disease can affect multiple organs, it primarily affects the lungs and occurs most frequently in adults. The risk of progression to active disease is greatest within the first two years following infection. TB incidence varies substantially across regions, with the highest rates reported in sub-Saharan Africa and Southeast Asia [62].

Chronic hepatitis C virus (HCV) infection is a major global health burden. As reported by the WHO, an estimated 50 million people currently live with chronic HCV, with approximately 1 million new infections occurring annually [35, 60]. In 2022, the disease was responsible for approximately 242,000 deaths, mainly due to complications, such as liver cirrhosis and hepatocellular carcinoma. Despite the availability of highly effective curative treatments, gaps in diagnosis and treatment coverage persist, posing major challenges to achieving global hepatitis C elimination goals [30, 52].

The coexistence of TB and HCV infection is both biologically and epidemiologically plausible, supported by extensive evidence of overlapping risk factors, immunological interactions, and clinical co-infection cases. Both diseases are prevalent in populations affected by poverty, overcrowding, limited healthcare access, and among high-risk groups such as individuals who inject drugs, the homeless, and immunocompromised individuals. A systematic review and meta-analysis reported that TB patients have significantly higher odds of HCV infection than the general population [7], while HCV infection independently increases the risk of developing active TB [8, 36]. Immunologically, HCV suppresses T-cell mediated responses essential for TB control, reducing TB-specific CD4 responses thereby facilitating TB progression [23]. Partial or incomplete treatment arising from poor diagnosis, such as addressing only one infection while neglecting the other, further exacerbates the burden of TB–HCV co-infection. Undiagnosed or untreated HCV during TB therapy increases susceptibility to drug-induced hepatotoxicity, leading to treatment interruptions or defaults, which compromise TB control and extend the infectious period [37, 55]. However, treating HCV without TB screening may permit TB reactivation, given the immune dysregulation caused by chronic viral infection. The WHO emphasizes that the simultaneous management of TB and HCV is feasible and necessary, as delayed or selective treatment undermines therapeutic success for both diseases.

A range of mathematical modeling frameworks has been developed to analyze the transmission dynamics and control strategies of TB and HCV infections. Egonmwan and Okuonghae [21] formulated a model assessing the impact of diagnosis and treatment for both latent and active TB, indicating backward bifurcation, sensitivity to key epidemiological parameters, and the potential to reduce the TB burden through improved detection and treatment. Avilov and Romanyuka [3] incorporated antituberculosis programs into a model differentiating between detected and undetected cases, revealing significant disparities in TB morbidity and detection efficiency

Math. Open 2026.05. Downloaded from www.worldscientific.com
by 196.43.164.50 on 11/12/26. Re-use and distribution is strictly not permitted, except for Open Access articles.

across regions. Kasereka *et al.* [33] developed an eight-compartment model showing that rapidly progressing latent cases drive short- and medium-term incidences, while slowly progressing latent cases sustain long-term persistence. Their findings underscored the importance of interventions, such as contact tracing and latent case treatment for effective TB control. Khajanchi *et al.* [34] showed that exogenous reinfection and endogenous reactivation significantly influence TB dynamics, with backward and Hopf bifurcations indicating that the basic reproduction below one may not guarantee disease elimination. The study [17] developed a TB transmission model incorporating social awareness and media interventions. The analysis revealed backward bifurcation and showed that media awareness influences TB transmission and disease persistence. Optimal control results demonstrated that sustained media intervention can reduce TB prevalence. In [31], a fractional-order two-patch TB model incorporating exogenous reinfection and human movement was developed. The study showed that population movement and fractional-order dynamics influence TB prevalence, with backward bifurcation occurring under certain conditions. Numerous other modeling studies have further explored TB transmission and intervention strategies [5, 14, 18, 25, 42, 44, 46, 47], while systematic reviews [16, 58], have synthesized recent advances and highlighted persistent challenges, including disease reactivation and relapse.

In the case of HCV, Elbasha [22] emphasized the role of reinfection and critical epidemiological parameters, showing that high-efficacy treatment can substantially reduce disease burden. The model in [2] used a threshold parameter to predict treatment outcomes from early viral dynamics. Martin *et al.* [38] demonstrated that infection risk and injection duration among IDUs are the primary determinants of the required treatment level, whereas immunity status has little effect, supporting treatment as a preventive measure. Okosun and Makinde [48] applied optimal control theory and concluded that prioritizing the treatment of acutely and chronically infected individuals is most cost-effective in resource limited-settings, while broader screening and treatment programs could further improve outcomes at a higher cost. The impact of alcohol abuse on the progression of HCV infection was examined in [40], where findings indicated that reduced alcohol consumption lowers the risk of progression to chronic infection and improves treatment outcomes. Furthermore, a sex-structured model of HCV transmission among people who inject drugs [29] demonstrated that gender specific behaviors and needle-related factors play a significant role in driving transmission, with harm reduction strategies being essential for effective control. Additionally, a compartmental HCV model incorporating awareness-based susceptible classes and optimal control [53] revealed that the simultaneous implementation of multiple intervention strategies substantially reduced disease transmission, as supported by both stability and simulation analyses.

Despite growing evidence of TB–HCV co-infection, mathematical models addressing their joint dynamics remain scarce. Notably, Kizito *et al.* [35] developed one of the few existing models, focusing on co-infection dynamics in the absence of

interventions and establishing linear relationships between key infected compartments and transmission parameters. In contrast, a substantial body of literature has examined co-infections involving either TB or HCV, such as HIV–HCV [1, 9, 19, 24, 51], TB–HIV [4, 10, 50], and TB–COVID-19 [41]. Collectively, these studies highlight the importance of integrated modeling approaches but do not explicitly address the unique epidemiological and treatment complexities of TB–HCV co-infection.

To address this gap, this study proposes a novel and comprehensive deterministic modeling framework that extends existing approaches in several important ways. First, unlike prior TB–HCV models, the proposed model explicitly incorporates partial treatment, capturing the realistic effects of incomplete or inadequate therapy due to delayed diagnosis, poor adherence, or limited healthcare access. Second, the model integrates dual treatment dynamics, allowing for the simultaneous management of TB and HCV infections and enabling the assessment of their combined therapeutic impact. Third, this study formulates and analyzes an optimal control problem that jointly considers TB and HCV awareness, detection, and treatment interventions, an aspect not addressed in earlier TB–HCV co-infection models.

2. Model Description and Formulation

2.1. *Description of the model*

The model categorizes the human population into 13 distinct and separate groups ascending to their epidemiological status, namely, susceptible individuals capable of acquiring TB or HCV ($S(t)$), latently infected individuals with TB who are not contagious ($T_L(t)$), infectious individuals with TB who are contagious ($T_I(t)$), infectious individuals with TB who are hospitalized ($T_H(t)$), recovered from TB individuals ($T_R(t)$), infectious individuals with acute HCV who are not symptomatic ($H_A(t)$), HCV chronically infectious individuals with symptoms ($H_C(t)$), recovered from HCV individuals ($H_R(t)$), dually infected with acute HCV infection and non-infectious latent TB ($C_1(t)$), dually infected with chronic HCV and non-infectious latent TB ($C_2(t)$), dually infected with acute HCV infection and infectious TB ($C_3(t)$), dually infected with chronic HCV and infectious TB ($C_4(t)$), and individuals who have recovered from the co-infection ($R(t)$).

Treatment for HCV patients is initiated at the chronic stage, as the acute stage is generally brief and asymptomatic, while diagnosis commonly takes place during the persistent and symptomatic chronic phase of infection [39]. To formulate the dynamic system, it is assumed that all susceptible individuals have equal risk of acquiring either TB or HCV, with transmission occurring through contact with infectious individuals. Individuals who recover from TB or HCV infection following treatment are assumed to gain temporary immunity before eventually returning to the susceptible class. The overall population in the community at any time t was

Math. Open 2026.05. Downloaded from www.worldscientific.com
by 196.43.164.50 on 11/12/26. Re-use and distribution is strictly not permitted, except for Open Access articles.

defined as follows:

$$N(t) = S(t) + T_L(t) + T_I(t) + T_H(t) + T_R(t) + H_A(t) + H_C(t) + H_T(t) + C_1(t) + C_2(t) + C_3(t) + C_4(t) + R(t).$$

The susceptible population, $S(t)$, receives a continuous inflow through births and immigration at a rate Λ, and all sub-populations are subject to a constant natural mortality rate, denoted by μ. Susceptible individuals acquire TB infection and transition to the latent TB class, T_L, at a force of infection β_T, which is defined as follows:

$$\beta_T = \frac{\lambda p(T_I(t) + qT_H(t) + b_1 C_3(t) + b_2 C_4(t))}{N(t)}. \tag{1}$$

Here, λ denotes the inter-personal contact rate between TB-infectious and susceptible individuals, and p is the probability that a contact results in TB transmission. The parameter q represents the reduced risk of TB transmission from hospitalized individuals, attributable to the effects of intensive care. Parameters b_1 and b_2 are enhancement factors accounting for the elevated risk of TB transmission from dually infected individuals in classes C_3 and C_4, respectively. These factors capture the fact that dually infected individuals transmit TB more efficiently than those infected with TB alone, due to a higher pathogen load [4, 35]. It was further assumed that $b_2 > b_1$.

Susceptible individuals acquire HCV infection and transition to acute class $I_A(t)$, at a force of infection $\beta_H(t)$, defined by

$$\beta_H(t) = \frac{\xi k(mH_A(t) + H_C(t) + m_1 C_1(t) + m_2 C_2(t) + m_3 C_3(t) + m_4 C_4(t))}{N(t)}. \tag{2}$$

The parameter ξ denotes the rate of human-to-human contact between HCV-infected and susceptible individuals. The chance that such contact results in HCV transmission is represented by k. The parameters $m_i, i = 1, 2, 3, 4$ serve as enhancement factors that capture the increased risk of HCV transmission from dually infected individuals in classes C_1, C_2, C_3, and C_4, respectively. Furthermore, m was introduced as an amplification parameter to account for the comparatively higher risk of transmission from individuals acutely infected with HCV.

Humans latently infected with TB, T_L, may either recover naturally due to an improved immune response at a rate ε, thereby returning to the susceptible class, or progress to active TB infection, T_I, at a rate σ. Individuals with active TB who are diagnosed as positive may follow two treatment pathways: a proportion are managed at home under treatment at a rate δ_1, transitioning to the recovery class T_R, while others are hospitalized at a rate θ, entering compartment T_H. Hospitalized patients also receive treatment, and upon recovery at a rate δ_2, they join the recovery class T_R.

Math. Open 2026.05. Downloaded from www.worldscientific.com
by 196.43.164.50 on 11/12/26. Re-use and distribution is strictly not permitted, except for Open Access articles.

Math. Open 2026.05. Downloaded from www.worldscientific.com
by 196.43.164.50 on 11/12/26. Re-use and distribution is strictly not permitted, except for Open Access articles.

Individuals acutely infected with HCV, may either recover naturally at a rate γ, then return to the susceptible class, or progress to chronic HCV infection, H_C, at a rate α. Upon successful diagnosis of chronic HCV, infected individuals are initiated on treatment at a rate ρ, after which they transition to recovery class H_R. Latently and actively infected individuals with TB, represented by T_L and T_I, may acquire HCV through a force of infection β_H, thereby transitioning to dual-infection classes C_1 and C_3, respectively. Conversely, individuals acutely and chronically infected with HCV, denoted by H_A and H_C, may acquire TB through a force of infection β_T, progressing to dual-infection classes C_1 and C_2, respectively.

Individuals in the dual infection class C_1 may progress either to active TB and acute HCV class C_3 at a rate τ_2 or to latent TB and chronic HCV class C_2 at a rate τ_1. Likewise, transitions into HCV chronic and infectious TB co-infection class $C_4(t)$ occur from $C_2(t)$ and $C_3(t)$ at rates τ_3 and τ_4, respectively.

Partial treatment of the co-infected individuals was also considered. Specifically, individuals in C_2 may receive treatment for HCV at a rate ρ, thereby reverting to the latent TB class; individuals in C_3 may be treated for TB at a rate δ_1, moving into the acute HCV class; and individuals in C_4 may either be treated for TB at a rate δ_1, transitioning to the chronic HCV class, or be treated for HCV at a rate ρ, reverting to the active TB class. Furthermore, once diagnosed as positive for both infections, individuals in C_3 and C_4 may be placed on dual therapy at rates π_1 and π_2, respectively, ultimately progressing into the recovered class $R(t)$.

Since previous infection does not confer permanent immunity, individuals in the recovery classes T_R, H_R, and $R(t)$ representing those treated for TB, HCV, and dual infection, respectively may revert to the susceptible class after clearance of infection. This occurs at rates ν_1, ν_2, and ν, respectively.

Individuals in the community face disease-induced mortality, occurring at rates d_1 and d_2 for classes T_H and T_I respectively; at rate d for the chronic HCV class; and rates c_1 and c_2 for co-infection classes C_3 and C_4, respectively.

2.2. *Compartmental diagram*

A schematic of the TB–HCV co-infection model, represented as a compartmental diagram, is shown in Fig. 1.

2.3. *Parameters of the model and their description*

Table 1 lists the parameters of the model and their description. Parameter values were estimated from WHO [60, 61], Uganda National Tuberculosis and Leprosy Programme (NTLP) annual reports [56], World Bank demographic indicators [59], and published HCV studies in sub-Saharan Africa.

Math. Open 2026.05. Downloaded from www.worldscientific.com
by 196.43.164.50 on 11/12/26. Re-use and distribution is strictly not permitted, except for Open Access articles.

Table 1. Parameters used in the model formulation and their description.

Parameter	Definition	Value (year^{-1})	Source
Λ	Per capita recruitment rate into susceptible population	$0.0352N_0$	Estimated
λ	Per susceptible risky contact rate for TB	730	Estimated
p	Probability that a risky contact results in TB infection	0.0026	Estimated
ξ	Per susceptible risky exposure rate for HCV	1.00	Estimated
k	Probability of HCV transmission per risky exposure	0.01	Estimated
q	Relative transmissibility of hospitalized TB cases	0.05–0.50	Estimated
μ	Natural mortality rate	0.01465	Estimated
d_1, d_2	Infectious TB-induced death rates in classes T_H and T_I	0.13,0.05	Estimated
d	Chronic HCV-induced death rate	0.03	Estimated
c_1, c_2	Co-infection induced death rates in classes C_3 and C_4	0.18,0.25	Estimated
σ	Rate of progression from latent to infectious TB	0.10	[43]
θ	Hospitalization rate of TB infectious individuals	0.20	Estimated
δ_1	Treatment rate of TB infectious individuals	2.00	Estimated
δ_2	Treatment rate of TB hospitalized infectious individuals	4.00	Estimated
α	Transition rate from acute HCV to chronic HCV	1.60	[28]
τ_1	Transition rate from C_1 class to C_2 class	1.00	Assumed
τ_2	Transition rate from C_1 class to C_3 class	0.80	Assumed
τ_3	Transition rate from C_2 class to C_4 class	1.00	Assumed
τ_4	Transition rate from C_3 class to C_4 class	1.00	Assumed
ρ	Treatment rate of chronically infected HCV individuals	0.10	Estimated
π_1, π_2	Dual treatment in co-infected individuals C_3 and C_4	0.05, 0.10	Assumed
ν	Progression rates to susceptible class after recovery in R	0.50	Estimated
ν_1	Progression rates to susceptible class after recovery in T_R	1.00	Estimated
ν_2	Progression rates to susceptible class after recovery in H_R	1.00	Estimated
ε	Natural recovery rate of latent TB in T_L class	0.01	[43]
γ	Natural recovery rate of acute HCV in H_A class	0.45	[28]

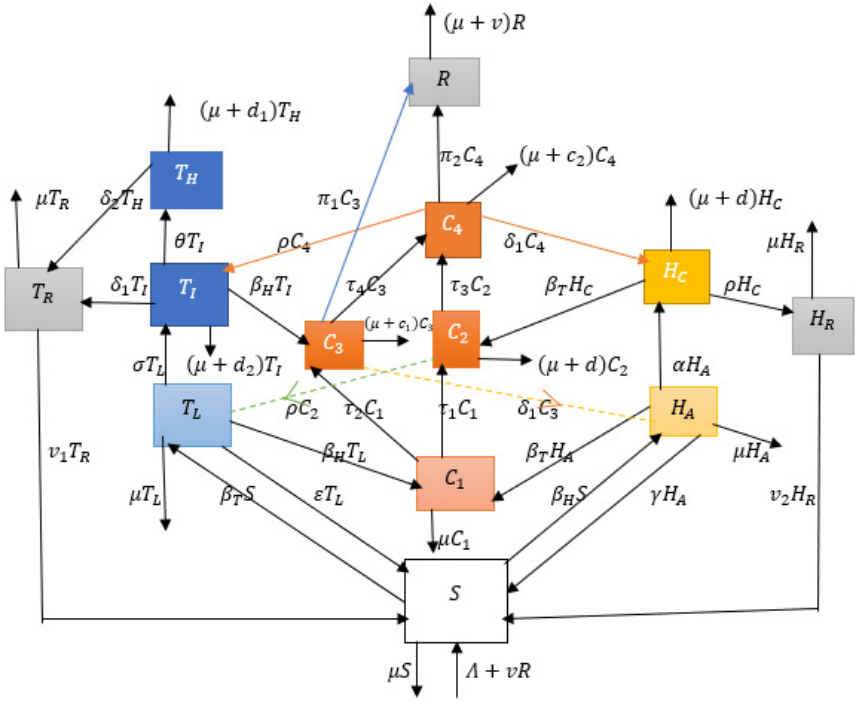


Fig. 1. A Flow diagram for the co-dynamics of TB and HCV.

Math. Open 2026.05. Downloaded from www.worldscientific.com
by 196.43.164.50 on 11/12/26. Re-use and distribution is strictly not permitted, except for Open Access articles.

2.4. *Equations of the model*

Based on Fig. 1 and the model description, the system is described by the following set of ordinary differential equations:

$$\begin{aligned}
\frac{dS}{dt} &= \Lambda + \nu R + \nu_1 T_R + \nu_2 H_R + \varepsilon T_L + \gamma H_A - (\beta_T + \beta_H + \mu)S,\\
\frac{dT_L}{dt} &= \beta_T S + \rho C_2 - (\beta_H + \varepsilon + \sigma + \mu)T_L,\\
\frac{dT_I}{dt} &= \sigma T_L + \rho C_4 - (\beta_H + \delta_1 + \theta + \mu + d_2)T_I,\\
\frac{dT_H}{dt} &= \theta T_I - (\delta_2 + \mu + d_1)T_H,\\
\frac{dT_R}{dt} &= \delta_1 T_I + \delta_2 T_H - (\nu_1 + \mu)T_R,\\
\frac{dH_A}{dt} &= \beta_H S + \delta_1 C_3 - (\beta_T + \gamma + \alpha + \mu)H_A,\\
\frac{dH_C}{dt} &= \alpha H_A + \delta_1 C_4 - (\beta_T + \rho + \mu + d)H_C,\\
\frac{dH_R}{dt} &= \rho H_C - (\nu_2 + \mu)H_R,\\
\frac{dC_1}{dt} &= \beta_T H_A + \beta_H T_L - (\tau_1 + \tau_2 + \mu)C_1,\\
\frac{dC_2}{dt} &= \beta_T H_C + \tau_1 C_1 - (\rho + \tau_3 + \mu + d)C_2,\\
\frac{dC_3}{dt} &= \beta_H T_I + \tau_2 C_1 - (\delta_1 + \pi_1 + \tau_4 + \mu + c_1)C_3,\\
\frac{dC_4}{dt} &= \tau_4 C_3 + \tau_3 C_2 - (\rho + \delta_1 + \pi_2 + \mu + c_2)C_4,\\
\frac{dR}{dt} &= \pi_1 C_3 + \pi_2 C_4 - (\nu + \mu)R.
\end{aligned} \tag{3}$$

The total population is not constant but varies over time and its dynamics are governed by the following differential equation:

$$\frac{dN}{dt} = \Lambda - \mu N - (d(H_C + C_2) + d_1 T_H + d_2 T_I + c_1 C_3 + c_2 C_4). \tag{4}$$

The state variables of the system are initially given by

$$\begin{cases}
S(0) > 0, \quad T_L(0) \geq 0, \quad T_I(0) \geq 0, \quad T_H(0) \geq 0, \quad T_R(0) \geq 0,\\
H_A(0) \geq 0, \quad H_C(0) \geq 0, \quad H_R(0) \geq 0, \quad C_1(0) \geq 0,\\
C_2(0) \geq 0, \quad C_3(0) \geq 0, \quad C_4(0) \geq 0, \quad \text{and} \quad R(0) \geq 0.
\end{cases} \tag{5}$$

3. Analysis of the Model

3.1. *Basic properties of the model with no controls*

Because model system (3) describes the dynamics of the human population, it is necessary to verify that it is both mathematically well posed and biologically meaningful. In this subsection, we examine the solution properties of TB-HCV co-infection model (3), with particular emphasis on positivity and boundedness.

Lemma 3.1. *For the non-negative initial conditions* (5)*, the solutions* $S, T_L, T_I, T_H, T_R, H_A, H_C, H_R, C_1, C_2, C_3, C_4$ *and* R *for model system* (3) *are non-negative for* $t \geq 0$.

Proof. To demonstrate the non-negativity of the systems' solutions, we proceed by contradiction. Suppose there exists a first time $t_1 > 0$ at which a state variable $S(t)$ reaches zero with a negative derivative, that is, $S(t_1) = 0$ and $S'(t_1) < 0$, whereas all other state variables remain non-negative for $0 < t < t_1$. Considering the corresponding differential equation of model system (3), we obtain

$$\frac{dS(t_1)}{dt} = \Lambda + \nu_1 T_R + \nu_2 H_R + \nu R + \epsilon T_L + \gamma H_A > 0.$$

This result contradicts the assumption that $S'(t_1) < 0$. Following the same procedure it can be seen that

$$\begin{cases} \frac{dT_L(t_2)}{dt} = \beta_T S + \rho C_2 \geq 0, \\ \frac{dT_I(t_3)}{dt} = \sigma T_L + \rho C_4 \geq 0, \\ \frac{dT_H(t_4)}{dt} = \theta T_H \geq 0, \\ \frac{dT_R(t_5)}{dt} = \delta_1 T_I + \delta_2 T_H \geq 0, \\ \frac{dH_A(t_6)}{dt} = \beta_H S + \delta_1 C_3 \geq 0, \\ \frac{dH_C(t_7)}{dt} = \alpha H_A + \delta_1 C_4 \geq 0, \\ \frac{dH_R(t_8)}{dt} = \rho H_C \geq 0, \\ \frac{dC_1(t_9)}{dt} = \beta_T H_A + \beta_H T_L \geq 0, \\ \frac{dC_2(t_{10})}{dt} = \beta_T H_A + \tau_1 C_1 \geq 0, \\ \frac{dC_3(t_{11})}{dt} = \beta_H T_I + \tau_2 C_1 \geq 0, \\ \frac{dC_4(t_{12})}{dt} = \tau_4 C_3 + \tau_3 C_2 \geq 0, \\ \frac{dC_5(t_{13})}{dt} = \pi_1 C_3 + \pi_2 C_4 \geq 0. \end{cases}$$

Therefore, no state variable can become negative, and it follows that all state solutions remain non-negative. □

Math. Open 2026.05. Downloaded from www.worldscientific.com
by 196.43.164.50 on 11/12/26. Re-use and distribution is strictly not permitted, except for Open Access articles.

Math. Open 2026.05. Downloaded from www.worldscientific.com
by 196.43.164.50 on 11/12/26. Re-use and distribution is strictly not permitted, except for Open Access articles.

It is also crucial to show that the model population is bounded and is within a region of biological significance. The following lemma represents the region in which system (3) is restricted.

Lemma 3.2. *The feasible region*

$$\Omega = \left\{ (S, T_L, T_I, T_H, T_R, H_A, H_C, H_R, C_1, C_2, C_3, C_4, R) \in \mathbb{R}_+^{13} : 0 \leq N(t) \leq \frac{\Lambda}{\mu} \right\} \quad (6)$$

is a positively invariant and attractive set with respect to model system (3).

Proof. The equation for the change in the total population (4) reduces to the inequality:

$$\frac{dN}{dt} \leq \Lambda - \mu N. \quad (7)$$

Applying the comparison theorem to inequality (7) with the initial condition $N(0) = N_0$, we derive that

$$N \leq \frac{\Lambda}{\mu} + \left(N_0 - \frac{\Lambda}{\mu} \right) e^{-\mu t}. \quad (8)$$

Thus, inequality (8) implies that

$$0 \leq N(t) \leq \frac{\Lambda}{\mu}.$$

Hence, the feasible region Ω is positively invariant and is attracted under the flow induced by system (3). Therefore, model (3) is well-posed in Ω and it is sufficient to study the dynamics of the model. □

3.2. *Disease-free equilibrium and the reproduction number*

The basic reproduction number, denoted by $\mathcal{R}$, represents the expected number of new infections generated by an infectious individual introduced into an entirely susceptible population [57]. To determine the reproduction number for the TB–HCV co-infection model, the next-generation matrix approach outlined in [20, 54, 57] was employed. By equating the right-hand side of system (3) to zero and substituting $T_L = T_I = T_H = H_A = H_C = C_1 = C_2 = C_3 = C_4 = 0$ in the absence of TB, HCV, and their co-infection, we obtain $T_R = H_R = R = 0$ and $S = \frac{\Lambda}{\mu}$. Consequently, the disease-free equilibrium point is given by

$$E_0 = \left(\frac{\Lambda}{\mu}, 0, 0, 0, 0, 0, 0, 0, 0, 0, 0, 0, 0 \right). \quad (9)$$

To derive the basic reproduction number, we focused on the infected compartments $T_L, T_I, T_H, H_A, H_C, C_1, C_2, C_3$, and C_4. Following the next-generation matrix approach,

Math. Open 2026.05. Downloaded from www.worldscientific.com
by 196.43.164.50 on 11/12/26. Re-use and distribution is strictly not permitted, except for Open Access articles.

we denote by F_i the rate of appearance of new infections in compartment i, and by V_i the rate of transfer of individuals into and out of compartment i through all other processes. The Jacobian matrices F and V whose entries are the partial derivatives of the new-infection terms F_i and the transition terms V_i with respect to the infected states are formed and evaluated at the disease-free equilibrium as follows:

$$F = \begin{bmatrix} 0 & \lambda p & \lambda pq & 0 & 0 & 0 & 0 & \lambda pb_1 & \lambda pb_2 \\ 0 & 0 & 0 & 0 & 0 & 0 & 0 & 0 & 0 \\ 0 & 0 & 0 & 0 & 0 & 0 & 0 & 0 & 0 \\ 0 & 0 & 0 & \xi km & \xi k & \xi km_1 & \xi km_2 & \xi km_3 & \xi km_4 \\ 0 & 0 & 0 & 0 & 0 & 0 & 0 & 0 & 0 \\ 0 & 0 & 0 & 0 & 0 & 0 & 0 & 0 & 0 \\ 0 & 0 & 0 & 0 & 0 & 0 & 0 & 0 & 0 \\ 0 & 0 & 0 & 0 & 0 & 0 & 0 & 0 & 0 \\ 0 & 0 & 0 & 0 & 0 & 0 & 0 & 0 & 0 \end{bmatrix},$$

$$V = \begin{bmatrix} k_1 & 0 & 0 & 0 & 0 & 0 & 0 & 0 & 0 \\ -\sigma & k_2 & 0 & 0 & 0 & 0 & 0 & 0 & -\rho \\ 0 & -\theta & k_3 & 0 & 0 & 0 & 0 & 0 & 0 \\ 0 & 0 & 0 & k_4 & 0 & 0 & 0 & 0 & 0 \\ 0 & 0 & 0 & -\alpha & k_5 & 0 & 0 & 0 & -\delta_1 \\ 0 & 0 & 0 & 0 & 0 & k_6 & 0 & 0 & 0 \\ 0 & 0 & 0 & 0 & 0 & -\tau_1 & k_7 & 0 & 0 \\ 0 & 0 & 0 & 0 & 0 & -\tau_2 & 0 & k_8 & 0 \\ 0 & 0 & 0 & 0 & 0 & 0 & -\tau_3 & -\tau_4 & k_9 \end{bmatrix}, \tag{10}$$

where $k_1 = (\varepsilon + \sigma + \mu), k_2 = (\delta_1 + \theta + \mu + d_2), k_3 = (\delta_2 + \mu + d_1), k_4 = (\gamma + \alpha + \mu)$, $k_5 = (\rho + \mu + d), k_6 = (\tau_1 + \tau_2 + \mu), k_7 = (\rho + \tau - 1 + \tau_2 + \mu), k_8 = (\delta_1 + \pi_1 + \tau_4 + \mu + c_1)$, and $k_9 = (\rho + \delta_1 + \pi_2 + \mu + c_2)$. The next-generation matrix is $K = FV^{-1}$ and the basic reproduction number is the spectral radius of K which in this case is given by

$$\mathcal{R} = \max\{\mathcal{R}_T, \mathcal{R}_H\}, \tag{11}$$

where

$$\begin{aligned} \mathcal{R}_T &= \frac{\lambda p\sigma(\delta_2 + \mu + d_1 + q\theta)}{(\varepsilon + \sigma + \mu)(\delta_1 + \theta + \mu + d_2)(\delta_2 + \mu + d_1)}, \\ \mathcal{R}_H &= \frac{\xi k(m(\rho + \mu + d) + \alpha)}{(\gamma + \alpha + \mu)(\rho + \mu + d)}. \end{aligned} \tag{12}$$

The quantities $\mathcal{R}_T$ and $\mathcal{R}_H$ denote the basic reproduction numbers corresponding to the TB-only and HCV-only sub-models, respectively.

In this context, $\mathcal{R}$ is defined as the expected number of new TB or HCV infections generated by a single individual infected with TB, HCV, or both when introduced

into a wholly susceptible population. According to [57, Theorem 2], the following result is obtained.

Theorem 3.3. *The disease-free equilibrium* (9) *of system* (3) *is locally asymptotically stable when* $\mathcal{R} < 1$ *and unstable otherwise.*

3.3. *Existence of the endemic equilibrium point*

Owing to the nonlinear and complex nature of the co-infection model (3), the existence of an endemic equilibrium point was established through the analysis of the TB and HCV sub-models. Furthermore, the overall co-infection dynamics were determined by the behavior of these sub-models. The corresponding TB and HCV sub-models were obtained as follows:

TB sub-model

$$\begin{aligned}
\frac{dS}{dt} &= \Lambda + \nu_1 T_R + \varepsilon T_L - (\beta_T + \mu)S,\\
\frac{dT_L}{dt} &= \beta_T S + (\varepsilon + \sigma + \mu)T_L,\\
\frac{dT_I}{dt} &= \sigma T_L + (\delta_1 + \theta + \mu + d_2)T_I,\\
\frac{dT_H}{dt} &= \theta T_I - (\delta_2 + \mu + d_1)T_H,\\
\frac{dT_R}{dt} &= \delta_1 T_I + \delta_2 T_H - (\nu_1 + \mu)T_R,
\end{aligned} \tag{13}$$

where $\beta_T = \lambda p(\frac{T_I + qT_H}{N_T})$ is the TB-only infection force.

HCV sub-model

$$\begin{aligned}
\frac{dS}{dt} &= \Lambda + \nu_2 H_R + \gamma H_A - (\beta_H + \mu)S,\\
\frac{dH_A}{dt} &= \beta_H S - (\gamma + \alpha + \mu)H_A,\\
\frac{dH_C}{dt} &= \alpha H_A - (\rho + \mu + d)H_C,\\
\frac{dH_R}{dt} &= \rho H_C - (\nu_2 + \mu)H_R,
\end{aligned} \tag{14}$$

where $\beta_H = \xi k(\frac{mH_A + H_C}{N_H})$ is the HCV-only infection force.

The endemic equilibrium point corresponding to system (13) is obtained as $E_T = (S^*, T_L^*, T_I^*, T_H^*, T_R^*)$, where $S^* = \frac{N_T^* k_1 k_2 k_3}{\lambda p \sigma (k_3 + q\theta)}$, $T_L^* = \frac{\beta_T^* S^*}{k_1}$, $T_I^* = \frac{\sigma \beta_T^* S^*}{k_1 k_2}$, $T_H^* = \frac{\theta \sigma \beta_T^* S^*}{k_1 k_2 k_3}$, $T_R^* = \frac{\sigma \beta_T^* S^* (\delta_1 k_4 + \delta_2 \theta)}{k_1 k_2 k_3 k_4}$, $\beta_T^* = \frac{\lambda p \sigma k_4 (k_3 + q\theta)\Lambda - N_T^* \mu k_1 k_2 k_3 k_4}{k_1 k_2 k_3 k_4 - \nu_1 \sigma (\delta_1 k_3 + \delta_2 \theta) - \varepsilon k_2 k_3 k_4}$, $k_1 = (\varepsilon + \sigma + \mu)$, $k_2 = (\theta + \mu + d_2 + \delta_1)$, $k_3 = (\mu + d_1 + \delta_2)$, and $k_4 = (\nu_1 + \mu)$.

Math. Open 2026.05. Downloaded from www.worldscientific.com by 196.43.164.50 on 11/12/26. Re-use and distribution is strictly not permitted, except for Open Access articles.

Math. Open 2026.05. Downloaded from www.worldscientific.com
by 196.43.164.50 on 11/12/26. Re-use and distribution is strictly not permitted, except for Open Access articles.

The endemic equilibrium point corresponding to system (14) is obtained as $E_H = (S^*, H_A^*, H_C^*, H_R^*)$, where $S^* = \frac{N_H^* q_1 q_2}{\xi k(mq_2+\alpha)}, H_A^* = \frac{\beta_H^* S^*}{q_1}$, $H_C^* = \frac{\alpha\beta_H^* S^*}{q_1 q_2}$, $H_R^* = \frac{\rho\alpha\beta_H^* S^*}{q_1 q_2 q_3}$, $\beta_H^* = \frac{\xi k q_1 q_3 \Lambda(q_2 m+\alpha)-\mu q_1 q_2 q_3}{q_1 q - 2q_3 - \nu_2\rho\alpha - \gamma q_2 q_3}$, $q_1 = (\gamma+\alpha+\mu), q_2 = (\rho+\mu+d)$, and $q_3 = (\nu_2+\mu)$.

Lemma 3.4. *A unique endemic equilibrium E_T exists for the TB sub-model (13) if and only if the basic reproduction number satisfies $\mathcal{R}_T > 1$.*

Proof. For TB endemicity, $\frac{dT_L}{dt} > 0, \frac{dT_I}{dt} > 0$, and $\frac{dT_H}{dt} > 0$, implying that

$$\lambda p(T_I + qT_H)\frac{S}{N_T} + (\varepsilon+\sigma+\mu)T_L > 0, \tag{15}$$

$$\sigma T_L + (\delta_1+\theta+\mu+d_2)T_I > 0, \tag{16}$$

$$\theta T_I - (\delta_2+\mu+d_1)T_H > 0. \tag{17}$$

At any time t, $\frac{S}{N_T} \leq 1$ and inequality (15) becomes

$$T_L < \frac{\lambda p}{(\varepsilon+\sigma+\mu)}(T_I + qT_H). \tag{18}$$

Re-arranging inequalities (16) and (17) leads to

$$T_I < \frac{\sigma T_L}{(\delta_1+\theta+\mu+d_2)}, \tag{19}$$

$$T_H < \frac{\theta T_I}{(\delta_2+\mu+d_1)}. \tag{20}$$

Substituting inequalities (19) and (20) into (18) and simplifying leads to

$$1 < \frac{\lambda p\sigma(\delta_2+\mu+d_1+q\theta)}{(\varepsilon+\sigma+\mu)(\delta_1+\theta+\mu+d_2)(\delta_2+\mu+d_1)} = \mathcal{R}_T.$$

Hence, E_T is unique when $\mathcal{R}_T > 1$. □

Lemma 3.5. *A unique endemic equilibrium E_H exists for the HCV sub-model (14) if and only if the basic reproduction number satisfies $\mathcal{R}_H > 1$.*

Proof. For persistence of HCV in a community, $\frac{dH_A}{dt} > 0, \frac{dH_C}{dt} > 0$, translating to

$$\xi k(mH_A + H_C)\frac{S}{N_H} - (\gamma+\alpha+\mu)H_A > 0, \tag{21}$$

$$\alpha H_A - (\rho+\mu+d)H_C > 0. \tag{22}$$

Given that $\frac{S}{N_H} \leq 1$, inequality (21) reduces to

$$H_A < \frac{\xi k(mH_A + H_C)}{(\gamma+\alpha+\mu)}. \tag{23}$$

Making H_C a subject in inequality (22) and substituting the result into (23), leads to

$$1 < \frac{\xi k(m(\rho+\mu+d)+\alpha)}{(\gamma+\alpha+\mu)(\rho+\mu+d)} = \mathcal{R}_H.$$

Hence, E_H is unique when $\mathcal{R}_H > 1$. □

Because the TB and HCV sub-models admit unique endemic equilibrium points, E_T and E_H, whenever $\mathcal{R}_T > 1$ and $\mathcal{R}_H > 1$, respectively, it follows that the full TB–HCV co-infection model also admits a unique endemic equilibrium $E = (S^*, T_L^*, T_I^*, T_H^*, T_R^*, H_A^*, H_C^*, H_R^*, C_1^*, C_2^*, C_3^*, C_4^*, R^*)$ whenever $\mathcal{R} > 1$. This outcome is consistent with the findings in [35, 54], which demonstrate that the overall dynamics of co-infection systems are largely governed by the underlying behavior of their constituent sub-models. Consequently, the existence and persistence of the endemic state in the coupled model were directly linked to the transmission potential within each individual disease component, thereby justifying the following result.

Theorem 3.6. *The TB-HCV endemic state of system* (3) *is locally asymptotically stable when* $\mathcal{R} > 1$ *and unstable otherwise.*

3.4. *Sensitivity analysis of the basic reproduction number*

A sensitivity analysis was conducted to identify the key parameters that influence the transmission dynamics of TB, HCV, and their co-infection, as well as the effectiveness of corresponding infection control interventions within the community. The normalized sensitivity index of a variable with respect to a given parameter is defined as the ratio of the relative change in the variable to the relative change in that parameter [11, 51]. Accordingly, the normalized sensitivity index of the basic reproduction number $\mathcal{R}$, with respect to any given parameter p^*, is expressed as follows:

$$\mathcal{D}_{p^*}^{\mathcal{R}} = \frac{\partial \mathcal{R}}{\partial p^*} \times \frac{p^*}{\mathcal{R}}. \tag{24}$$

Table 2. Sensitivity indices for $\mathcal{R}_T$.

Parameter	Sensitivity index
λ	+1.0000
p	+1.0000
q	+0.0096
σ	+0.1978
μ	−0.1240
d_1	-2.9982×10^{-4}
d_2	−0.0221
θ	−0.0788
δ_1	−0.8831
δ_2	−0.0092
ε	−0.0802

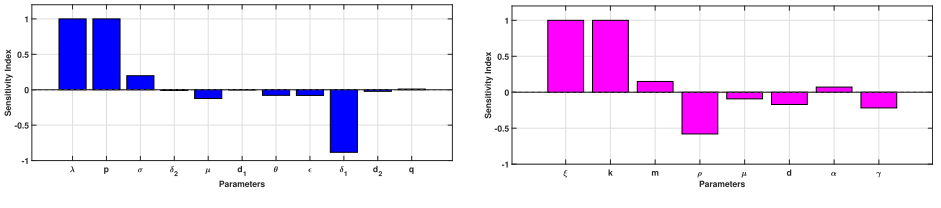
Math. Open 2026.05. Downloaded from www.worldscientific.com
by 196.43.164.50 on 11/12/26. Re-use and distribution is strictly not permitted, except for Open Access articles.

Table 3. Sensitivity indices for $\mathcal{R}_H$.

Parameter	Sensitivity index
ξ	+1.0000
k	+1.0000
m	+0.1531
α	+0.0719
μ	−0.0929
d	−0.11756
γ	−0.2180
ρ	−0.5855

Because the overall co-infection basic reproduction number, $\mathcal{R}$, is determined by the basic reproduction numbers of the TB and HCV sub-models, denoted by $\mathcal{R}_T$ and $\mathcal{R}_H$, respectively, the sensitivity indices were computed for each sub-model separately. Tables 2 and 3 present the normalized sensitivity indices of $\mathcal{R}_T$ and $\mathcal{R}_H$, respectively, calculated using Eq. (24) and the parameter values provided in Table 1.

Sensitivity indices in Tables 2 and 3 were used to obtain Fig. 2. Figure 2(a) shows that the per susceptible risky contact rate (λ) and the probability that a risky contact results in TB infection (p) both have sensitivity indices of +1.0000, implying that a 1% increase in either of these parameters causes an equivalent 1% increase in $\mathcal{R}_T$, making them highly influential parameters for TB transmission. In the context of TB–HCV co-infection, high values of λ and p can also enhance the risk of dual infection, since individuals with HCV-induced immunosuppression may be more susceptible to TB. The progression rate from latent to infectious TB (σ) also positively influenced $\mathcal{R}_T$. This suggests that individuals who progress more rapidly from latent infection to active TB contributed substantially to spread of the disease. The relative transmissibility of hospitalized TB cases (q) has a small positive effect, indicating that infection control measures in hospitals can minimize the spread of TB among hospitalized individuals. The hospitalization rate of infectious TB individuals (θ) also contributes to control by isolating infectious individuals from susceptible individuals, thereby limiting exposure opportunities. Most notably, the treatment rate of infectious TB individuals (δ_1) shows a strong negative sensitivity index, signifying that treatment has a profound impact on reducing TB transmission and



(a) Sensitivity indices of $\mathcal{R}_T$. (b) Sensitivity indices of $\mathcal{R}_H$.

Fig. 2. Sensitivity indices of the basic reproduction number parameters.

Math. Open 2026.05. Downloaded from www.worldscientific.com by 196.43.164.50 on 11/12/26. Re-use and distribution is strictly not permitted, except for Open Access articles.

consequently the co-infection risk. The treatment rate of hospitalized TB cases (δ_2) had a weaker effect, implying that interventions should prioritize early treatment before hospitalization.

Similarly, Fig. 2(b) indicates that the per susceptible risky exposure rate (ξ) and the probability of HCV transmission per exposure (k) exert the strongest positive effects on $\mathcal{R}_H$. Parameter m moderately increases $\mathcal{R}_H$ implying that acute HCV-infected individuals contribute to HCV transmission. The transition rate from acute to chronic HCV infection (α) also has a small positive effect, indicating that progression to chronic stages sustains long term infectivity, thereby maintaining disease persistence. Negative sensitivity indices were observed for several parameters, indicating their contributions to the control of TB–HCV co-infection. The natural recovery rate of acute HCV infection (γ) and the treatment rate of chronically infected HCV individuals (ρ) substantially reduce $\mathcal{R}_H$ which is important in reducing co-infection.

4. Formulation of the Optimal Control Problem

Optimal control strategies for managing TB–HCV co-infection, a persistent global health challenge, were investigated using mathematical modeling and optimal control theory. We analyzed co-infection dynamics and evaluated interventions such as treatment, screening, and community awareness to identify strategies that minimize disease burden and inform public health policies. We applied Pontryagin's maximum principle [12, 49] to determine the optimal interventions for TB–HCV co-infection. This approach uses the Hamiltonian and adjoint equations derived from system dynamics to identify control functions that minimize the disease burden. Optimal control methods have been successfully applied to infectious disease models, including TB, HCV, HIV, and pneumonia [4, 11–13, 48]. In this study, the following time-dependent control functions were introduced into the TB–HCV co-infection model (3) to evaluate the optimal effort required to reduce transmission and disease burden.

(a) TB awareness control, denoted by $u_1(t)$, represents a preventive strategy aimed at reducing the risk of TB infection in the susceptible population. Its implementation may be achieved through targeted health education campaigns designed to raise awareness of TB and its implications within the context of TB-HCV co-infection.

(b) TB detection and treatment control, denoted by $u_2(t)$, are designed to facilitate the timely identification and effective management of individuals exposed to or infected with TB. This strategy encompasses active case finding, use of rapid diagnostic tools, adherence support through directly observed therapy, and reinforcement of healthcare delivery systems.

Math. Open 2026.05. Downloaded from www.worldscientific.com
by 196.43.164.50 on 11/12/26. Re-use and distribution is strictly not permitted, except for Open Access articles.

(c) HCV awareness control, denoted by $u_3(t)$, is a preventive strategy intended to lower the risk of HCV infection among the susceptible population. It is implemented through educational initiatives that disseminate information on preventive measures and encourage responsible health seeking behaviors among both susceptible and already infected individuals.

(d) HCV detection and treatment control, denoted by $u_4(t)$, is a strategy aimed at identifying and managing individuals infected with HCV through timely therapeutic interventions. This approach is implemented by ensuring prompt initiation of antiviral therapy for all individuals who test positive for HCV, thereby reducing the risk of disease progression and transmission.

Considering the control measures described above, model system (3) can be rewritten as follows:

$$\begin{aligned}
\frac{dS}{dt} &= \Lambda + \nu R + \nu_1 T_R + \nu_2 H_R + \varepsilon T_L + \gamma H_A - ((1-u_1)\beta_T + (1-u_3)\beta_H + \mu)S,\\
\frac{dT_L}{dt} &= (1-u_1)\beta_T S + (u_4+\rho)C_2 + u_4 C_1 - ((1-u_3)\beta_H + u_2 + \varepsilon + \sigma + \mu)T_L,\\
\frac{dT_I}{dt} &= \sigma T_L + (u_4+\rho)C_4 - ((1-u_3)\beta_H + (u_2+\delta_1) + \theta + \mu + d_2)T_I,\\
\frac{dT_H}{dt} &= \theta T_I - (\delta_2 + \mu + d_1)T_H,\\
\frac{dT_R}{dt} &= (u_2+\delta_1)T_I + \delta_2 T_H + u_2 T_L - (\nu_1 + \mu)T_R,\\
\frac{dH_A}{dt} &= (1-u_3)\beta_H S + (u_2+\delta_1)C_3 + u_2 C_1 + u_2 C_2 - ((1-u_1)\beta_T + u_4 + \gamma\\
&\quad + \alpha + \mu)H_A,\\
\frac{dH_C}{dt} &= \alpha H_A + (u_2+\delta_1)C_4 - ((1-u_1)\beta_T + (u_4+\rho) + \mu + d)H_C,\\
\frac{dH_R}{dt} &= (u_4+\rho)H_C + u_4 H_A - (\nu_2+\mu)H_R,\\
\frac{dC_1}{dt} &= (1-u_1)\beta_T H_A + (1-u_3)\beta_H T_L - (u_2 + u_4 + \tau_1 + \tau_2 + \mu)C_1,\\
\frac{dC_2}{dt} &= (1-u_1)\beta_T H_C + \tau_1 C_1 - ((u_4+\rho) + u_2 + \tau_3 + \mu + d)C_2,\\
\frac{dC_3}{dt} &= (1-u_3)\beta_H T_I + \tau_2 C_1 - ((u_2+\delta_1) + (u_2+u_4+\pi_1) + \tau_4 + \mu + c_1)C_3,\\
\frac{dC_4}{dt} &= \tau_4 C_3 + \tau_3 C_2 - ((u_4+\rho) + (u_2+\delta_1) + (u_2+u_4+\pi_2) + \mu + c_2)C_4,\\
\frac{dR}{dt} &= (u_2+u_4+\pi_1)C_3 + (u_2+u_4+\pi_2)C_4 - (\nu+\mu)R.
\end{aligned} \tag{25}$$

Math. Open 2026.05. Downloaded from www.worldscientific.com
by 196.43.164.50 on 11/12/26. Re-use and distribution is strictly not permitted, except for Open Access articles.

Math. Open 2026.05. Downloaded from www.worldscientific.com
by 196.43.164.50 on 11/12/26. Re-use and distribution is strictly not permitted, except for Open Access articles.

4.1. *The control system*

For system (25), the goal is to minimize both the number of infected, and co-infected individuals and the cost of the implemented control measures. The objective function to be minimized is given by

$$Z(u_1,u_2,u_3,u_4) = \int_0^{t_f} (A_1T_L + A_2T_I + A_3H_A + A_4H_C + A_5C_1 + A_6C_2 + A_7C_3 + A_8C_4 + \frac{1}{2}\sum_{i=1}^{4} B_i u_i^2\Big)dt \tag{26}$$

subject to model (25), where u_1, u_2, u_3, and u_4 are *Lebesgue* measurable and bounded functions on $[0, t_f]$. The positive constants $A_i (i = 1, 2, \ldots, 8)$ and $B_i (i = 1, 2, 3, 4)$ serve as weighting parameters that balance the cost contributions from the state variables and control measures $T_L, T_I, H_A, H_C.C_1, C_2, C_3, C_4, u_1, u_2, u_3$, and u_4. The disease-related cost is assumed to be proportional to the number of infected individuals in each compartment, while the costs associated with the control strategies are modeled as nonlinear, specifically quadratic, consistent with previous [11, 32].

This study seeks the best strategy to control the dynamics of system (25). For this case, the optimal controls $u_1^*, u_2^*, u_3^*, u_4^*$ are required such that

$$Z(u_1^*, u_2^*, u_3^*, u_4^*) = \min_{u_1,u_2,u_3,u_4} \{Z(u_1,u_2,u_3,u_4) | (u_1,u_2,u_3,u_4) \in \mathcal{U}\}, \tag{27}$$

where the control set $\mathcal{U} = \{(u_1, u_2, u_3, u_4)$ such that u_1, u_2, u_3, u_4 are measurable with $[0, t_f] \to [0, 1]\}$.

4.2. *Existence of optimal control solutions*

The fundamental concern in this context is the existence of optimal control and the conditions under which it can be assured. The question is whether it is possible to guarantee the presence of a control strategy that minimizes a specified performance criterion. Establishing the existence of an optimal control is of critical importance because it ensures that the optimization problem is well-posed and that the pursuit of an optimal solution is both theoretically valid and practically meaningful.

Theorem 4.1. *There exists an optimal control quadruple* $\mathcal{U}^* = (u_1^*, u_2^*, u_3^*, u_4^*)$ *and solution vector* $X^* = (S^*, T_L^*, T_I^*, T_H^*, T_R^*, H_A^*, H_C^*, H_R^*, C_1^*, C_2^*, C_3^*, C_4^*, R^*)$ *corresponding to system* (25) *that minimizes the objective function* (26).

The nontrivial conditions pertaining to the set of admissible controls and terminal conditions, as outlined in [11, 26], are presented and verified as follows.

(1) The set of all solutions to Eqs. (25) and (26) and the corresponding control functions in $\mathcal{U}$ are non-empty.

(2) The state system (25) can be written as a linear function of the control variables with coefficients dependent on the time and state variables.
(3) The integrand Z in (26) of the objective function given by

$$Z(X,u,t) = A_1T_L + A_2T_I + A_3H_A + A_4H_C + A_5C_1 + A_6C_2 + A_7C_3 + A_8C_4 + \frac{1}{2}\sum_{i=1}^{4} B_i \overset{2}{u}_i \tag{28}$$

is convex on Ω and also satisfies $Z(x,u,t) \geq \xi_1|(u_1,u_2,u_3,u_4)|^\beta - \xi_2$, where $\xi_1 > 0$ and $\beta > 1$.

Proof. To verify condition 1, we apply the Picard−Lindelöf theorem [27], which guarantees the existence of a unique solution for every admissible control $\mathcal{U}$, provided that the state equations are continuous and Lipschitz continuous in the state variables. Because the total population is bounded below by a positive constant N_0 and above by $\frac{\Lambda}{\mu}$ as outlined in Lemma 3.2 all state variables, which are subsets of the total population, are likewise bounded. This implies that the state system is continuous with bounded partial derivatives with respect to the state variables. Therefore, Condition 1 is satisfied.

Condition 2 is verified by noting that the state equations depend linearly on control variables u_1, u_2, u_3, and u_4. This linear dependence satisfies the regularity conditions required for an optimal control.

To verify Condition 3, we refer to the definition of convex functions in [6], which states that any constant or polynomial of degree two is convex. Hence objective function $Z(X,u,t)$ is convex on the set of admissible controls $\mathcal{U}$.

Next, we establish the boundedness of $Z(X,u,t)$. Because each control $u_i \in [0,1]$ for $i = 1,2,3,4$, it follows that:

$$B_4u_4^2 \leq B_4 \;\Rightarrow\; \frac{1}{2}B_4u_4^2 \leq \frac{B_4}{2} \;\Rightarrow\; \frac{1}{2}B_4u_4^2 - \frac{B_4}{2} \leq 0.$$

Because all A_i and B_i are positive constants, Eq. (28) leads to the inequality

$$Z(X,u,t) \geq \frac{1}{2}(B_1u_1^2 + B_2u_2^2 + B_3u_3^2 + B_4u_4^2) - \frac{B_4}{2}. \tag{29}$$

Inequality (29) can be further simplified as follows:

$$Z(X,u,t) \geq \min\left(\frac{B_1}{2}, \frac{B_2}{2}, \frac{B_3}{2}, \frac{B_4}{2}\right)(\overset{2}{u}_1 + u_2^2 + u_3^2 + u_4^2) - \frac{B_4}{2}. \tag{30}$$

Letting $\xi_1 = \min(\frac{B_1}{2}, \frac{B_2}{2}, \frac{B_3}{2}, \frac{B_4}{2})$, $\xi_2 = \frac{B_4}{2}$, and $\beta = 2$, inequality (30) leads to

$$Z(X,u,t) \geq \xi_1||(u_1,u_2,u_3,u_4)||^\beta - \xi_2.$$

Thus, $Z(X,u,t)$ is both convex and bounded below, satisfying Condition 3.

Math. Open 2026.05. Downloaded from www.worldscientific.com
by 196.43.164.50 on 11/12/26. Re-use and distribution is strictly not permitted, except for Open Access articles.

Therefore, all required conditions were met, proving the existence of an optimal control solution. □

4.3. *Characterization of optimal control solution*

Pontryagin's maximum principle [11, 13, 49] was applied to characterize the optimal control strategies that minimize the spread of TB–HCV co-infection. This principle provides the necessary conditions for optimality, transforming the state system in system (25) and Eq. (26) into a pointwise minimization problem of the Hamiltonian function $\mathcal{H}$ with respect to control variables u_1, u_2, u_3, and u_4. The analysis examined adjoint dynamics, switching points, and cost constraints, offering insights into the structure of optimal interventions. Let $P_i; i = 1, 2, \ldots, 13$ be the adjoint functions or costate variables associated with the evolution of the corresponding state variables. Each of the adjoint functions is multiplied by the right-hand side of Eq. (25) defining the evolution of the corresponding state variable to obtain the Hamiltonian:

$$\begin{aligned}
\mathcal{H} = {} & A_1T_L + A_2T_I + A_3H_A + A_4H_C + A_5C_1 + A_6C_2 + A_7C_3 + A_8C_4 + \frac{1}{2}\sum_{i=1}^{4} B_i \overset{2}{u}_i \\
& + P_1(\Lambda + \nu R + \nu_1 T_R + \nu_2 H_R + \varepsilon T_L + \gamma H_A - ((1-u_1)\beta_T \\
& + (1-u_3)\beta_H + \mu)S) \\
& + P_2((1-u_1)\beta_T S + (u_4+\rho)C_2 + u_4 C_1 - ((1-u_3)\beta_H + u_2 + \varepsilon + \sigma + \mu)T_L) \\
& + P_3(\sigma T_L + (u_4+\rho)C_4 - ((1-u_3)\beta_H + (u_2+\delta_1) + \theta + \mu + d_2)T_I) \\
& + P_4(\theta T_I - (\delta_2 + \mu + d_1)T_H) + P_5((u_2+\delta_1)T_I + \delta_2 T_H + u_2 T_L - (\nu_1 + \mu)T_R) \\
& + P_6((1-u_3)\beta_H S + (u_2+\delta_1)C_3 + u_2 C_1 + u_2 C_2 - ((1-u_1)\beta_T + u_4 + \gamma \\
& + \alpha + \mu)H_A) \\
& + P_7(\alpha H_A + (u_2+\delta_1)C_4 - ((1-u_1)\beta_T + (u_4+\rho) + \mu + d)H_C) \\
& + P_8((u_4+\rho)H_C + u_4 H_A - (\nu_2+\mu)H_R) \\
& + P_9((1-u_1)\beta_T H_A + (1-u_3)\beta_H T_L - (u_2 + u_4 + \tau_1 + \tau_2 + \mu)C_1) \\
& + P_{10}((1-u_1)\beta_T H_C + \tau_1 C_1 - ((u_4+\rho) + u_2 + \tau_3 + \mu + d)C_2) \\
& + P_{11}((1-u_3)\beta_H T_I + \tau_2 C_1 - ((u_2+\delta_1) + (u_2 + u_4 + \pi_1) + \tau_4 + \mu + c_1)C_3) \\
& + P_{12}(\tau_4 C_3 + \tau_3 C_2 - ((u_4+\rho) + (u_2+\delta_1) + (u_2 + u_4 + \pi_2) + \mu + c_2)C_4) \\
& + P_{13}((u_2 + u_4 + \pi_1)C_3 + (u_2 + u_4 + \pi_2)C_4 - (\nu + \mu)R). \qquad (31)
\end{aligned}$$

Using Pontryagin's maximum principle, the necessary conditions for optimal controls and corresponding state variables were derived. Accordingly, the optimal controls u_1^*, u_2^*, u_3^*, and u_4^* are obtained from these conditions, which are evaluated step-by-step as follows:

(1) Adjoint equations: Here, the Hamilitonian (31) is differentiated with respect to each of the state variables to obtain adjoint equations:

$$\frac{dP_i}{dt} = \frac{\partial \mathcal{H}}{\partial X_i}, \quad \text{where } i = 1, 2, \ldots, 13. \qquad (32)$$

Math. Open 2026.05. Downloaded from www.worldscientific.com by 196.43.164.50 on 11/12/26. Re-use and distribution is strictly not permitted, except for Open Access articles.

Math. Open 2026.05. Downloaded from www.worldscientific.com
by 196.43.164.50 on 11/12/26. Re-use and distribution is strictly not permitted, except for Open Access articles.

The following equations are obtained from (32)

$$\begin{aligned}
\frac{dP_1}{dt} &= (1-u_1)\beta_T(P_1-P_2)+(1-u_3)\beta_H(P_1-P_6)+P_1\mu,\\
\frac{dP_2}{dt} &= (1-u_3)\beta_H(P_2-P_9)+u_2(P_2-P_5)+\varepsilon(P_2-P_1)+\sigma(P_2-P_3)\\
&\quad +\mu P_2-A_1,\\
\frac{dP_3}{dt} &= (1-u_1)\lambda p\left(\frac{S}{N}(P_1-P_2)+\frac{H_A}{N}(P_6-P_9)+\frac{H_C}{N}(P_7-P_{10})\right)\\
&\quad +(1-u_3)\beta_H(P_3-P_{11})+(u_2+\delta_1)(P_3-P_5)+\theta(P_3-P_4)\\
&\quad +(\mu+d_2)P_3-A_2,\\
\frac{dP_4}{dt} &= (1-u_1)q\lambda p\left(\frac{S}{N}(P_1-P_2)+\frac{H_A}{N}(P_6-P_9)+\frac{H_C}{N}(P_7-P_{10})\right)\\
&\quad +\delta_2(P_4-P_5)+(\mu+d_1)P_4,\\
\frac{dP_5}{dt} &= \nu_1(P_5-P_1)+\mu P_5,\\
\frac{dP_6}{dt} &= (1-u_3)\xi km\left(\frac{S}{N}(P_1-P_6)+\frac{T_L}{N}(P_2-P_9)+\frac{T_I}{N}(P_3-P_{11})\right)\\
&\quad +(1-u_1)\beta_T(P_6-P_9)+u_4(P_6-P_8)+\gamma(P_6-P_1)\\
&\quad +\alpha(P_6-P_7)+\mu P_6-A_3,\\
\frac{dP_7}{dt} &= (1-u_3)\xi k\left(\frac{S}{N}(P_1-P_6)+\frac{T_L}{N}(P_2-P_9)+\frac{T_I}{N}(P_3-P_{11})\right)\\
&\quad +(1-u_1)\beta_T(P_7-P_{10})+(u_4+\rho)(P_5-P_8)+\mu P_5-A_4,\\
\frac{dP_8}{dt} &= \nu_2(P_5-P_1)+\mu P_5,\\
\frac{dP_9}{dt} &= (1-u_3)\xi km_1\left(\frac{S}{N}(P_1-P_6)+\frac{T_L}{N}(P_2-P_9)+\frac{T_I}{N}(P_3-P_{11})\right)\\
&\quad +u_4(P_9-P_4)+u_2(P_9-P_6)+\tau_1(P_9-P_{10})+\tau_2(P_9-P_{11})\\
&\quad +\mu P_9-A_5,\\
\frac{dP_{10}}{dt} &= (1-u_3)\xi km_2\left(\frac{S}{N}(P_1-P_6)+\frac{T_L}{N}(P_2-P_9)+\frac{T_I}{N}(P_3-P_{11})\right)\\
&\quad +(u_4+\rho)(P_{10}-P_2)+u_2(P_{10}-P_6)+\tau_3(P_{10}-P_{12})\\
&\quad +(\mu+d)P_{10}-A_6,\\
\frac{dP_{11}}{dt} &= (1-u_1)\lambda pb_1\left(\frac{S}{N}(P_1-P_2)+\frac{H_A}{N}(P_6-P_9)+\frac{H_C}{N}(P_7-P_{10})\right)\\
&\quad +(1-u_3)\xi km_3\left(\frac{S}{N}(P_1-P_6)+\frac{T_L}{N}(P_2-P_9)+\frac{T_I}{N}(P_3-P_{11})\right)\\
&\quad +(u_2+\delta_1)(P_{11}-P_6)+\tau_4(P_{11}-P_{12})+(\mu+c_1)P_{11}\\
&\quad +(u_2+u_4+\pi_1)(P_{11}-P_{13})-A_7,
\end{aligned}$$

Math. Open 2026.05. Downloaded from www.worldscientific.com by 196.43.164.50 on 11/12/26. Re-use and distribution is strictly not permitted, except for Open Access articles.

$$\begin{aligned}\frac{dP_{12}}{dt} &= (1-u_1)\lambda p b_2\left(\frac{S}{N}(P_1-P_2)+\frac{H_A}{N}(P_6-P_9)+\frac{H_C}{N}(P_7-P_{10})\right)\\ &\quad+(1-u_3)\xi k m_4\left(\frac{S}{N}(P_1-P_6)+\frac{T_L}{N}(P_2-P_9)+\frac{T_I}{N}(P_3-P_{11})\right)\\ &\quad+(u_4+\rho)(P_{12}-P_3)+(u_2+\delta_1)(P_{12}-P_4)\\ &\quad+(u_2+u_4+\pi_2)(P_{12}-P_{13})+(\mu+c_2)P_{12}-A_8,\\ \frac{P_{13}}{dt} &= \nu(P_{13}-P_1)+\mu P_{13}. \end{aligned} \tag{33}$$

(2) The transversality conditions are obtained from

$$P_i(t_f)=0; \quad \text{for } i=1,2,3,4,5,6,7,8,9,10,11,12,13. \tag{34}$$

(3) The characterization of optimal controls is given by

$$\frac{\partial \mathcal{H}}{\partial u_1}=\frac{\partial \mathcal{H}}{\partial u_2}=\frac{\partial \mathcal{H}}{\partial u_3}=\frac{\partial \mathcal{H}}{\partial u_4}=0. \tag{35}$$

Equation (35) together with condition (34) leads to characterized controls

$$\begin{aligned} u_1^* &= \max\{0,\min\{1,\tau_1'\}\},\\ u_2^* &= \max\{0,\min\{1,\tau_2'\}\},\\ u_3^* &= \max\{0,\min\{1,\tau_3'\}\},\\ u_4^* &= \max\{0,\min\{1,\tau_4'\}\}, \end{aligned} \tag{36}$$

where

$$\begin{aligned} \tau_1' &= \frac{\beta_T S(P_2-P_1)+\beta_T H_A(P_9-P_6)+\beta_T H_C(P_{10}-P_7)}{B_1},\\ \tau_2' &= \frac{\begin{array}{l}T_L(P_2-P_5)+T_I(P_3-P_5)+C_1(P_9-P_6)+C_2(P_{10}-P_6)+C_3(2P_{11}\\ \quad -P_6-P_{13})+C_4(2P_{12}-P_7-P_{13})\end{array}}{B_2},\\ \tau_3' &= \frac{\beta_H S(P_6-P_1)+\beta_H T_L(P_9-P_2)+\beta_H T_I(P_{11}-P_3)}{B_3},\\ \tau_4' &= \frac{\begin{array}{l}H_A(P_6-P_8)+H_C(P_7-P_8)+C_1(P_9-P_2)+C_2(P_{10}-P_2)+C_3(P_{11}\\ \quad -P_{13})+C_4(2P_{12}-P_8-P_{13})\end{array}}{B_4}. \end{aligned} \tag{37}$$

From Eqs. (36) and (37), the control variables exhibit an inverse relationship with their corresponding cost functions. Given that the objective function is convex with respect to the control variables, and considering the boundedness of both the state and adjoint variables, it follows that the obtained optimal solution is unique for a sufficiently small final time t_f.

It is noteworthy that the optimal control variables and their corresponding state trajectories are determined by simultaneously solving the state system (25) subject to its initial conditions (4), adjoint system (33) with the associated transversality conditions (34), and characterization equations defining the optimal controls.

5. Numerical Simulations

The estimated parameter values used in the simulations are presented in Table 1. The total human population was estimated to be $N(0) = 45{,}600{,}000$, with initial compartment values specified as proportions of $N(0)$ based on available epidemiological data for TB and HCV in Uganda. Accordingly, the initial values are given as $S(0)= 39{,}819{,}000$, $T_L(0)= 4{,}377{,}600$ $T_I(0)= 45{,}144$, $T_H(0)=4{,}514$ $T_R(0) =91{,}200$, $H_A(0) = 45{,}600$, $H_C(0) = 342{,}000$, $H_R(0) = 91{,}200$, $C_1(0) = 43{,}776$, $C_2(0) = 32{,}832$, $C_3(0) = 45$, $C_4(0) = 338$, and $R(0)=22{,}800$.

The weights employed in the objective function are estimated as $A_1 = 30, A_2 = 20, A_3= 15, A_4 = 10, A_5 = 45, A_6 = 30, A_7 = 40, A_8 = 25 B_1 = 20, B_2 = 25, B_3 = 15$, and $B_4 = 20$. The control variables $u_1(t), u_2(t), u_3(t)$, and $u_4(t)$ are constrained between 0 and 1, reflecting the assumed range of effectiveness for the respective intervention strategies.

5.1. *Implication of the basic reproduction number on TB–HCV co-infection*

Figure 3 demonstrates that when the basic reproduction number exceeds one, TB, HCV, and their co-infection persist in the population. Conversely, when it falls below one, the possibility of eradicating co-infection emerges.

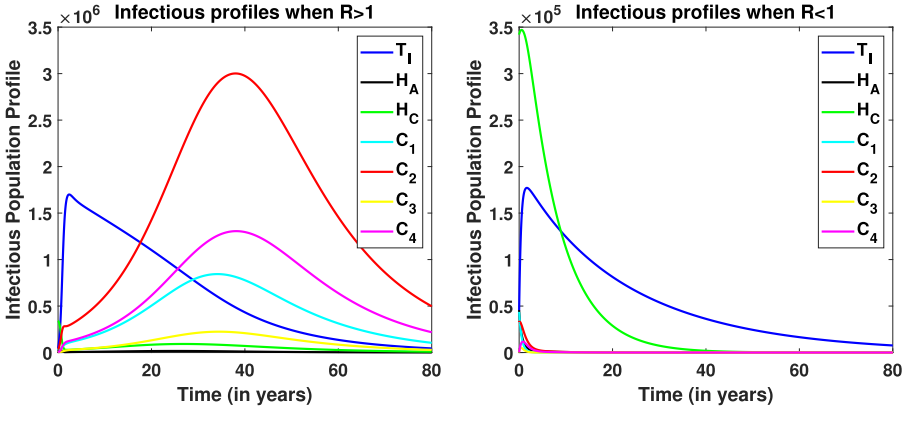


Fig. 3. Effect of $\mathcal{R}$ on TB–HCV co-dynamics.

Math. Open 2026.05. Downloaded from www.worldscientific.com by 196.43.164.50 on 11/12/26. Re-use and distribution is strictly not permitted, except for Open Access articles.

Math. Open 2026.05. Downloaded from www.worldscientific.com
by 196.43.164.50 on 11/12/26. Re-use and distribution is strictly not permitted, except for Open Access articles.

5.2. *Effect of treatment on the TB–HCV co-infection*

Since individuals co-infected with TB and HCV are not always simultaneously diagnosed with both infections but rather are often identified as having a single infection, we begin by examining the dynamics of TB–HCV co-infection in a scenario where only one of the infections is addressed. Figure 4 demonstrates that adherence to TB-based treatment alone effectively reduced the number of co-infected individuals, leading to the near elimination of co-infection after approximately four years of consistent intervention. In contrast, treatment strategies focused solely on HCV allow co-infection to persist within the community. This outcome highlights the dominant influence of TB on the overall dynamics of TB–HCV co-infection. Figure 4 further illustrates that simultaneous treatment with both TB and HCV is essential to reduce the overall burden of co-infection. This finding suggests that individuals diagnosed with either infection should undergo comprehensive screening to determine their status regarding the other, ensuring that appropriate treatment for both conditions concurrently is administered.

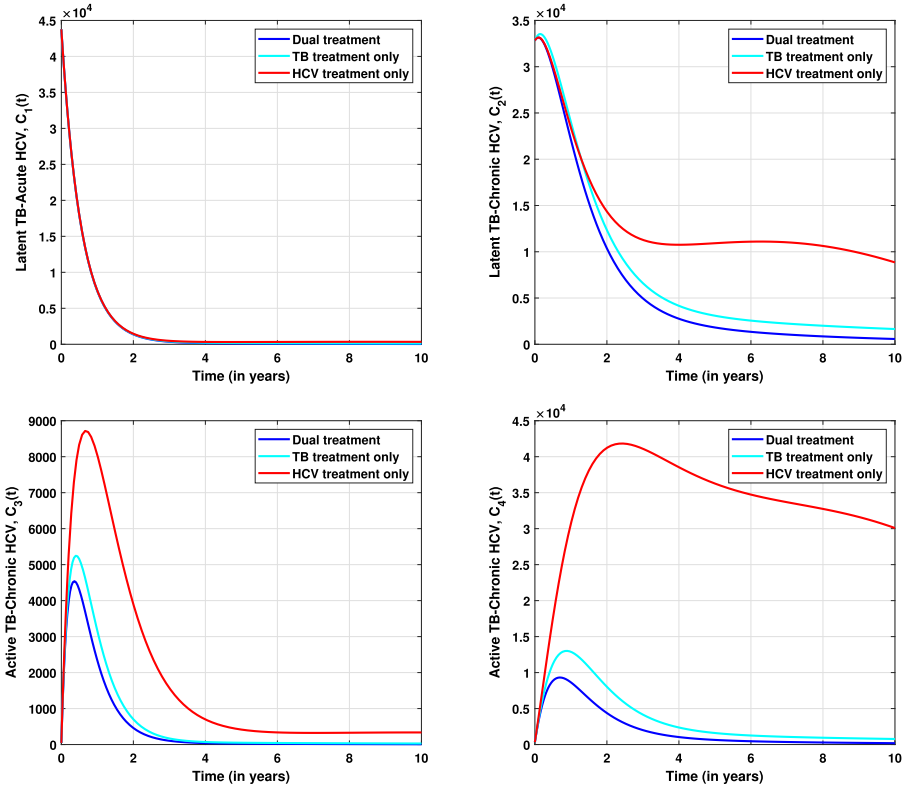


Fig. 4. Effect of partial treatment on TB-HCV co-infection.

Math. Open 2026.05. Downloaded from www.worldscientific.com
by 196.43.164.50 on 11/12/26. Re-use and distribution is strictly not permitted, except for Open Access articles.

5.3. *Effect of controls on the TB–HCV co-infection*

In this subsection, we assess the effectiveness of various combinations of control strategies on the dynamics of TB–HCV co-infection. The analysis considers the impact of individual control measures, pairwise combinations of two controls, combinations involving three controls, and simultaneous implementation of all control strategies.

The percentage reductions in co-infected individuals presented in Tables 4–6 are derived from the simulation results illustrated in Figs. 5, 7, and 8, respectively. The implementation of individual control strategies on the co-infected populations revealed that awareness efforts, u_1 for TB and u_3 for HCV, had the least impact on reducing TB–HCV co-infected individuals, as illustrated in Fig. 5. This observation is further supported by Table 4, which shows that implementing TB awareness campaigns resulted in percentage reductions of 5% in latent TB-acute HCV, 10% in

Table 4. Percentage reduction in co-infected individuals when a single control strategy is implemented.

Strategy	C_1	C_2	C_3	C_4
u_1	05	10	06	07
u_2	63	65	74	74
u_3	3.5	06	03	05
u_4	58	62	63	70

Table 5. Percentage reduction in co-infected individuals when a two-control strategy is implemented.

Strategy	C_1	C_2	C_3	C_4
$u_1 + u_2$	70	68	71	74
$u_1 + u_3$	15	16	14	10
$u_3 + u_4$	63	64	63	69
$u_2 + u_4$	80	82	84	85

Table 6. Percentage reduction in co-infected individuals when at least three controls are implemented.

Strategy	C_1	C_2	C_3	C_4
All controls	93	93	95	96
$u_1 + u_2 + u_3$	70	73	76	76
$u_1 + u_2 + u_4$	88	88	90	94
$u_1 + u_3 + u_4$	66	66	65	72
$u_2 + u_3 + u_4$	86	88	90	91

Math. Open 2026.05. Downloaded from www.worldscientific.com
by 196.43.164.50 on 11/12/26. Re-use and distribution is strictly not permitted, except for Open Access articles.

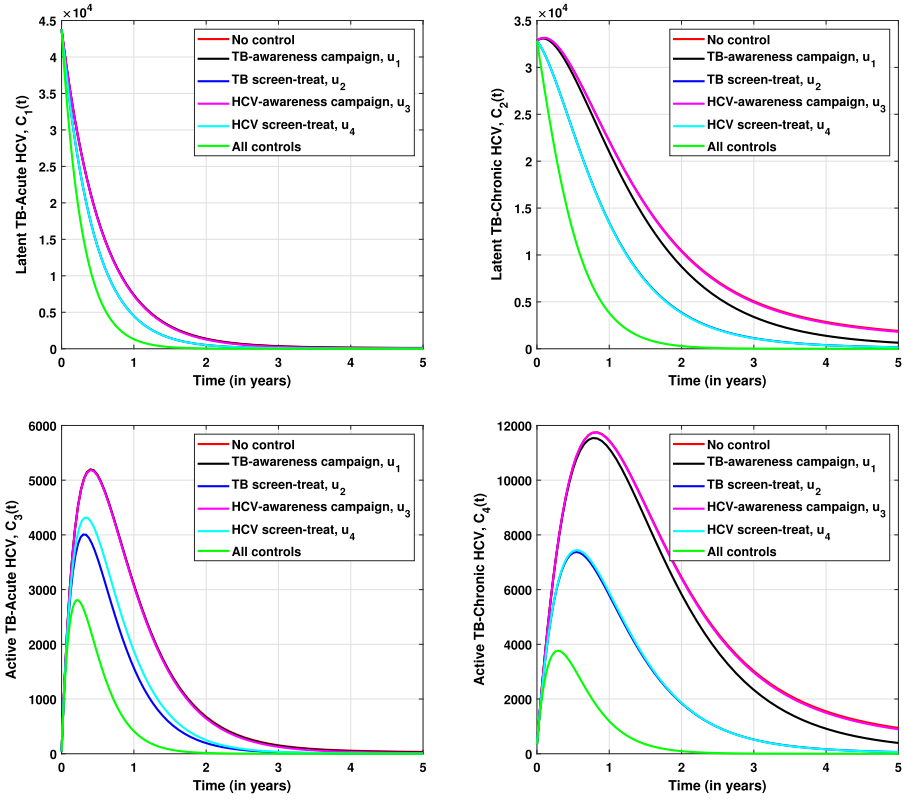


Fig. 5. Effect of a single control on TB–HCV co-infection.

latent TB–chronic HCV, 6% in active TB–acute HCV, and 7% in active TB–chronic HCV populations in 1.5 years. Figure 6 illustrates the impact of individual control measures on TB-only and HCV-only infections, showing the specific role of awareness, and detecting and treating interventions among singly infected populations. The results showed a consistent decline in both latently and actively TB-infected compartments following the implementation of awareness and treatment controls, in agreement with the findings reported in [45]. Similarly, the populations of acutely and chronically HCV-infected individuals exhibited a significant reduction when control measures u_3 and u_4 were applied, which is consistent with the results of [53]. The implementation of the two-control strategy illustrated in Fig. 7, demonstrated that the simultaneous application of detection and treatment interventions for both TB and HCV plays a pivotal role in reducing the co-infection burden compared to any other two-control combinations. This observation is supported by the results presented in Table 5, which indicate that combining the screen–treat interventions u_2 and u_4 for TB and HCV, respectively, resulted in percentage reductions of 80% in

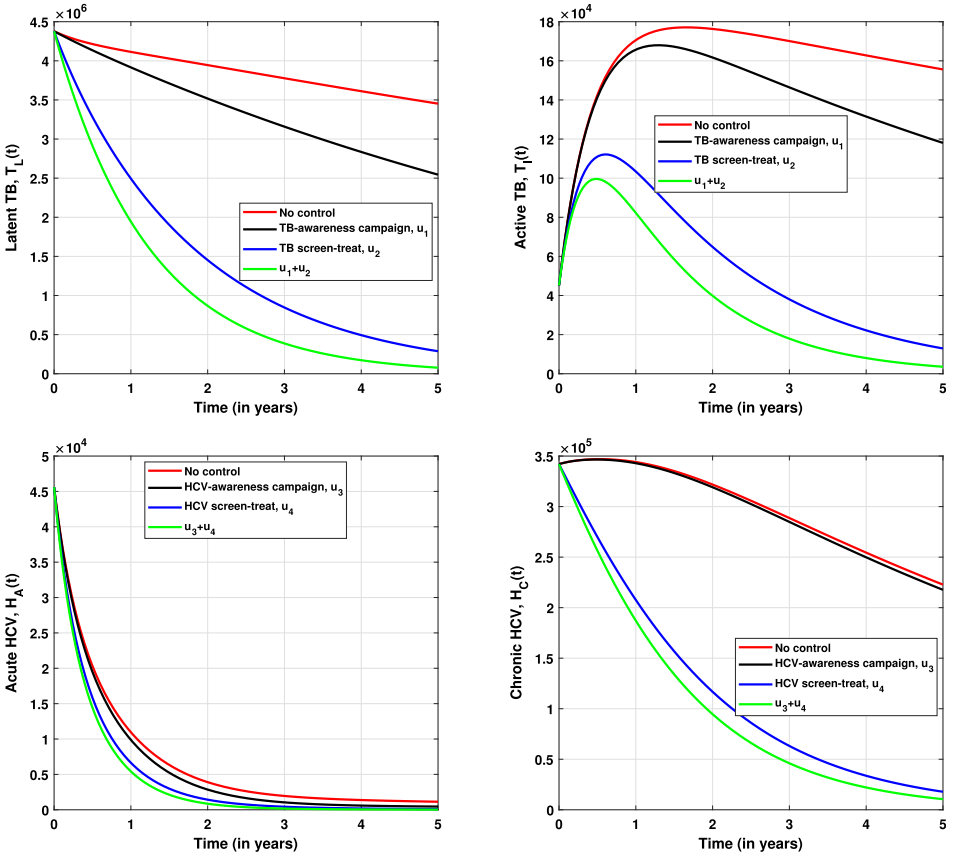


Fig. 6. Effect of controls on TB and HCV-only sub-models.

the latent TB–acute HCV, 82% in latent TB–chronic HCV, 84% in active TB–acute HCV, and 85% in active TB–chronic HCV populations.

Furthermore, as shown in Fig. 8, the implementation of the three-control strategy yields even more substantial reductions. Specifically, the combination of TB awareness campaigns with TB and HCV screening and treatment efforts produced reductions of 88% in both latent TB–acute HCV and latent TB–chronic HCV populations, 90% in active TB–acute HCV, and 94% in active TB–chronic HCV populations within approximately 1.5 years of implementation, as presented in Table 6.

The most pronounced impact, however, was observed when all control measures were implemented concurrently. This comprehensive approach led to reductions of 93% in latent TB–acute HCV, 93% in latent TB–chronic HCV, 95% in active TB–acute HCV, and 96% in active TB–chronic HCV populations within 1.5 years (Table 6).

Math. Open 2026.05. Downloaded from www.worldscientific.com
by 196.43.164.50 on 11/12/26. Re-use and distribution is strictly not permitted, except for Open Access articles.

Math. Open 2026.05. Downloaded from www.worldscientific.com
by 196.43.164.50 on 11/12/26. Re-use and distribution is strictly not permitted, except for Open Access articles.

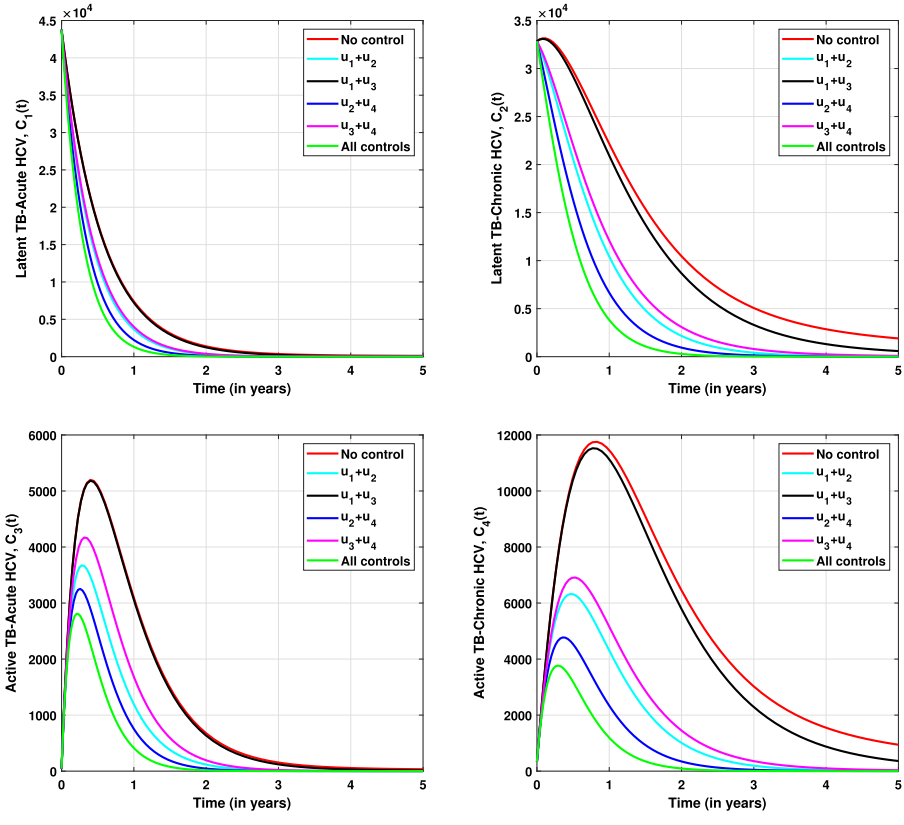
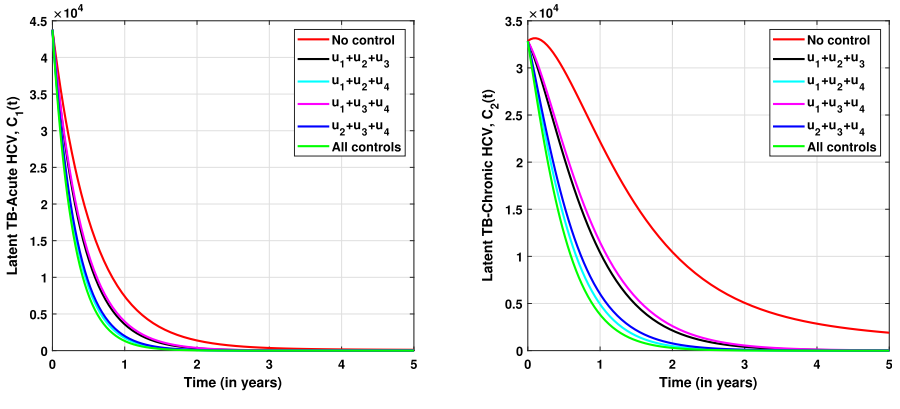
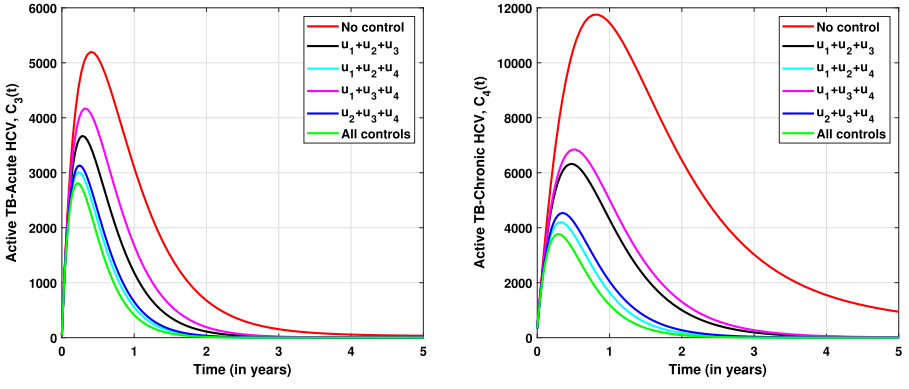


Fig. 7. Effect of combining two controls on TB–HCV co-infection.



(a)

Fig. 8. Effect of combining three controls on TB–HCV co-infection.



(b)

Fig. 8. (*Continued*)

Despite the effectiveness of the full control strategy, the associated costs were likely to be high. Therefore, the study findings suggest that prioritizing interventions targeting TB can yield substantial reductions in TB–HCV co-infection rates while maintaining cost-effectiveness.

6. Conclusion

This study developed and analyzed a mathematical model for TB–HCV co-infection incorporating four control strategies: TB awareness campaigns, TB screen–treat efforts, HCV awareness campaigns, and HCV screen–treat efforts. Sensitivity analysis identified the transmission parameters of both TB and HCV as the most influential in shaping co-infection dynamics, whereas treatment parameters were critical in reducing the reproduction numbers and overall co-infection burden. Numerical simulations showed that TB dominates co-infection, with TB-targeted treatment substantially reducing co-infection levels, although dual treatment targeting both infections proved to be more effective. These findings affirm not only the coexistence of TB and HCV but also highlight how partial treatment perpetuates a syndemic cycle of infection, increasing morbidity, mortality, and the overall co-infection burden, consistent with findings in [15]. Optimal control analysis using Pontryagin's maximum principle confirmed that the simultaneous implementation of all controls could nearly eradicate co-infection within two years. However, screening and treatment strategies for both infections, or TB awareness campaigns coupled with both TB and HCV screening and treatment, offered viable options.

Based on these findings, it is recommended that individuals diagnosed with either TB or HCV should be routinely screened for other infections to enable early detection

Math. Open 2026.05. Downloaded from www.worldscientific.com
by 196.43.164.50 on 11/12/26. Re-use and distribution is strictly not permitted, except for Open Access articles.

and concurrent treatment. Public health programs should prioritize TB-focused interventions along with integrated screening and treatment for both TB and HCV, as these strategies effectively reduce co-infection rates. Combining TB awareness campaigns with dual screening and treatment efforts can further enhance control outcomes, and implementing all measures simultaneously should be considered in high-burden settings with sufficient resources.

Math. Open 2026.05. Downloaded from www.worldscientific.com
by 196.43.164.50 on 11/12/26. Re-use and distribution is strictly not permitted, except for Open Access articles.

ORCID

Michael Byamukama https://orcid.org/0000-0002-1357-4797
Mohammed Kizito https://orcid.org/0000-0001-7737-7525

References

[1] O. E. Abiodun, O. Adebimpe, J. A. Ndako, O. Oludoun, B. Aladeitan and M. Adeniyi, Mathematical modeling of HIV-HCV co-infection model: Impact of parameters on reproduction number, *F1000Res.* **11** (2022) 1153.
[2] R. Avendaño, L. Esteva, J. A. Flores, J. F. Allen, G. Gómez and J. López-Estrada, A mathematical model for the dynamics of hepatitis C, *J. Theor. Med.* **4**(2) (2002) 109–118.
[3] K. K. Avilov and A. A. Romanyukha, Mathematical modeling of tuberculosis propagation and patient detection, *Autom. Remote Control* **68**(9) (2007) 1604–1617.
[4] T. K. Ayele, E. F. Doungmo Goufo and S. Mugisha, Co-infection mathematical model for HIV/AIDS and tuberculosis with optimal control in Ethiopia, *PLoS ONE* **19**(12) (2024) e0312539.
[5] A. Y. Ayinla, W. A. M. Othman and M. Rabiu, A mathematical model of the tuberculosis epidemic, *Acta Biotheor.* **69**(3) (2021) 225–255.
[6] V. Barbu and T. Precupanu, *Convexity and Optimization in Banach Spaces* (Springer Science & Business Media, 2012).
[7] M. Behzadifar, S. Heydarvand, M. Behzadifar and N. L. Bragazzi, Prevalence of hepatitis C virus in tuberculosis patients: A systematic review and meta-analysis, *Ethiop. J. Health Sci.* **29**(1) (2019) 945–956.
[8] U. Beijer, A. Wolf and S. Fazel, Prevalence of tuberculosis, hepatitis C virus, and HIV in homeless people: A systematic review and meta-analysis, *Lancet Infect. Dis.* **12**(11) (2012) 859–870.
[9] C. P. Bhunu and S. Mushayabasa, Modelling the transmission dynamics of HIV/AIDS and hepatitis C virus co-infection, *HIV AIDS Rev.* **12**(2) (2013) 37–42.
[10] B. Bolaji, T. Onoja, A. C. Benedict, B. I. Omede and U. B. Odionyenma, Dynamical analysis of HIV-TB co-infection transmission model in the presence of treatment for TB, *Bull. Biomath.* **2**(1) (2024) 21–56.
[11] M. Byamukama, D. Kajunguri and M. Karuhanga, Optimal control analysis of pneumonia and HIV/AIDS co-infection model, *Math. Open* **3** (2024) 2450006.
[12] M. Byamukama, M. Karuhanga and D. Kajunguri, Mathematical analysis of the role of treatment and vaccination in the management of the HIV/AIDS and pneumococcal pneumonia co-infection, *J. Math.* **2025**(1) (2025) 5879698.
[13] M. Byamukama and M. Kizito, Optimizing protection and treatment strategies for childhood pneumonia amid vaccine-unresponsive serotypes, *J. Appl. Math. Phys.* **13**(5) (2025) 1834–1857.

Math. Open 2026.05. Downloaded from www.worldscientific.com
by 196.43.164.50 on 11/12/26. Re-use and distribution is strictly not permitted, except for Open Access articles.

[14] C. Castillo-Chavez and B. Song, Dynamical models of tuberculosis and their applications, *Math. Biosci. Eng.* **1**(2) (2004) 361–404.
[15] A. Chua, L. Lim, S. H. Gan, C. Chee and Y. T. Wang, The role of chronic viral hepatitis on tuberculosis treatment interruption, *Int. J. Tuberc. Lung Dis.* **22**(12) (2018) 1486–1494.
[16] C. Colijn, T. E. D. Cohen and M. Murray, Mathematical models of tuberculosis: Accomplishments and future challenges, in *BIOMAT 2006: Int. Symp. Mathematical and Computational Biology* (World Scientific, Singapore, 2006), pp. 123–148.
[17] D. K. Das, S. Khajanchi and T. K. Kar, The impact of the media awareness and optimal strategy on the prevalence of tuberculosis, *Appl. Math. Comput.* **366** (2020) 124732.
[18] D. K. Das, S. Khajanchi and T. K. Kar, Transmission dynamics of tuberculosis with multiple re-infections, *Chaos Solitons Fractals* **130** (2020) 109450.
[19] F. Dayan, N. Ahmed, A. Bariq, A. Akgül, M. Jawaz, M. Rafiq and A. Raza, Computational study of a co-infection model of HIV/AIDS and hepatitis C virus models, *Sci. Rep.* **13**(1) (2023) 21938.
[20] A. Dwivedi, R. Keval and S. Khajanchi, Modeling optimal vaccination strategy for dengue epidemic model: A case study of India, *Phys. Scr.* **97**(8) (2022) 085214.
[21] A. O. Egonmwan and D. Okuonghae, Analysis of a mathematical model for tuberculosis with diagnosis, *J. Appl. Math. Comput.* **59**(1) (2019) 129–162.
[22] E. H. Elbasha, Model for hepatitis C virus transmissions, *Math. Biosci. Eng.* **10**(4) (2013) 1045–1065.
[23] M. A. El-Mokhtar *et al.*, Hepatitis C virus affects tuberculosis-specific T cells in HIV-negative patients, *Viruses* **12**(1) (2020) 101.
[24] T. S. Faniran, M. O. Adewole, H. Ahmad and F. A. Abdullah, Dynamics of tuberculosis in HIV-HCV co-infected cases, *Int. J. Biomath.* **16**(3) (2023) 2250091.
[25] F. Fatmawati, M. A. Khan, E. Bonyah, Z. Hammouch and E. M. Shaiful, A mathematical model of tuberculosis (TB) transmission with children and adults groups: A fractional model, *AIMS Math.* **5**(4) (2020) 2813–2842.
[26] W. H. Fleming and R. W. Rishel, *Deterministic and Stochastic Optimal Control*, Vol. 1 (Springer Science & Business Media, 2012).
[27] D. Grass, J. P. Caulkins, G. Feichtinger, G. Tragler and D. A. Behrens, *Optimal Control of Nonlinear Processes* (Springer, Berlin, 2008).
[28] B. Hajarizadeh, J. Grebely and G. J. Dore, Epidemiology and natural history of HCV infection, *Nat. Rev. Gastroenterol. Hepatol.* **10**(9) (2013) 553–562.
[29] M. Helikumi, J. Mushanyu and A. Mhlanga, A mathematical model of HCV transmission dynamics with sex stratification and environmental effects, *PLoS ONE* **20**(12) (2025) e0336374.
[30] W. Hladik *et al.*, Prevalence and screening costs of hepatitis C virus among Ugandan blood donors, *Trop. Med. Int. Health* **11**(6) (2006) 951–954.
[31] A. Jabbari, M. Lotfi, H. Kheiri and S. Khajanchi, Mathematical analysis of the dynamics of a fractional-order tuberculosis epidemic in a patchy environment under the influence of re-infection, *Math. Methods Appl. Sci.* **46**(17) (2023) 17798–17817.
[32] E. Jung, S. Lenhart and Z. Feng, Optimal control of treatments in a two-strain tuberculosis model, *Discrete Contin. Dyn. Syst. Ser. B* **2**(4) (2002) 473–482.
[33] S. Kasereka Kabunga, E. F. Doungmo Goufo and V. Ho Tuong, Analysis and simulation of a mathematical model of tuberculosis transmission in Democratic Republic of the Congo, *Adv. Differ. Equ.* **2020**(1) (2020) 642.
[34] S. Khajanchi, D. K. Das and T. K. Kar, Dynamics of tuberculosis transmission with exogenous reinfections and endogenous reactivation, *Physica A* **497** (2018) 52–71.

[35] M. Kizito, H. Nampala and P. Ariho, Mathematical modelling of tuberculosis and hepatitis C coinfection dynamics with no intervention, *J. Math.* **2024**(1) (2024) 5521979.
[36] A. V. Kukurika and I. A. Vasil'eva, Risk of drug-induced liver injury in patients with pulmonary tuberculosis and chronic viral hepatitis: Systematic review and meta-analysis, *Infect. Dis.: News Opin. Train.* **13**(2) (2024) 86–93.
[37] N. Lomtadze *et al.*, Hepatitis C virus co-infection increases the risk of anti-tuberculosis drug-induced hepatotoxicity among patients with pulmonary tuberculosis, *PLoS ONE* **8** (12) (2013) e83892.
[38] N. K. Martin, P. Vickerman and M. Hickman, Mathematical modelling of hepatitis C treatment for injecting drug users, *J. Theor. Biol.* **274**(1) (2011) 58–66.
[39] M. Martinello, B. Hajarizadeh, J. Grebely, G. J. Dore and G. V. Matthews, Management of acute HCV infection in the era of direct-acting antiviral therapy, *Nat. Rev. Gastroenterol. Hepatol.* **15**(7) (2018) 412–424.
[40] A. Mbeine Asiimwe, M. Byamukama and M. Karuhanga, Modeling the effect of alcohol consumption on the progression dynamics of hepatitis C infection with treatment, *Math. Med. Life Sci.* **3**(1) (2026) 2620745.
[41] K. G. Mekonen and L. L. Obsu, Mathematical modeling and analysis for the co-infection of COVID-19 and tuberculosis, *Heliyon* **8**(10) (2022) e11195.
[42] A. K. Mengistu and P. J. Witbooi, Mathematical analysis of TB model with vaccination and saturated incidence rate, *Abstr. Appl. Anal.* **2020** (2020) 1–10.
[43] N. A. Menzies *et al.*, Progression from latent infection to active disease in dynamic tuberculosis transmission models: A systematic review of the validity of modelling assumptions, *Lancet Infect. Dis.* **18**(8) (2018) e228–e238.
[44] L. N. Nkamba, T. T. Manga, F. Agouanet and M. L. Mann Manyombe, Mathematical model to assess vaccination and effective contact rate impact in the spread of tuberculosis, *J. Biol. Dyn.* **13**(1) (2019) 26–42.
[45] L. L. Obsu, Optimal control analysis of a tuberculosis model, *J. Biol. Syst.* **30**(4) (2022) 837–855.
[46] F. O. Ochieng, Mathematical modeling of tuberculosis transmission dynamics with reinfection and optimal control, *Eng. Rep.* **7**(1) (2025) e13068.
[47] M. M. Ojo, O. J. Peter, E. F. D. Goufo, H. S. Panigoro and F. A. Oguntolu, Mathematical model for control of tuberculosis epidemiology, *J. Appl. Math. Comput.* **69**(1) (2023) 69–87.
[48] K. O. Okosun and O. D. Makinde, Optimal control analysis of hepatitis C virus with acute and chronic stages in the presence of treatment and infected immigrants, *Int. J. Biomath.* **7**(2) (2014) 1450019.
[49] L. S. Pontryagin, *Mathematical Theory of Optimal Processes* (CRC Press, 1987).
[50] N. Raza, S. Irum, S. Niazai, M. A. Ullah, M. Y. Alshahrani and A. Omame, A mathematical framework of HIV and TB co-infection dynamics, *Sci. Rep.* **15**(1) (2025) 11465.
[51] A. Y. C. Sanchez, M. Aerts, Z. Shkedy, P. Vickerman, F. Faggiano, G. Salamina and N. Hens, A mathematical model for HIV and hepatitis C co-infection and its assessment from a statistical perspective, *Epidemics* **5**(1) (2013) 56–66.
[52] E. Seremba *et al.*, Poor performance of hepatitis C antibody tests in hospital patients in Uganda, *J. Med. Virol.* **82**(8) (2010) 1371–1378.
[53] S. W. Teklu, T. S. Lachamo and T. T. Guya, Analyses of a stage structure hepatitis C virus compartmental model with optimal control theory, *Model. Earth Syst. Environ.* **11** (2) (2025) 138.
[54] S. W. Teklu and B. B. Terefe, COVID-19 and syphilis co-dynamic analysis using mathematical modeling approach, *Front. Appl. Math. Stat.* **8** (2023) 1101029.

Math. Open 2026.05. Downloaded from www.worldscientific.com
by 196.43.164.50 on 11/12/26. Re-use and distribution is strictly not permitted, except for Open Access articles.

[55] A. Tostmann, M. J. Boeree, R. E. Aarnoutse, W. C. De Lange, A. J. Van Der Ven and R. Dekhuijzen, Antituberculosis drug-induced hepatotoxicity: Concise up-to-date review, *J. Gastroenterol. Hepatol.* **23**(2) (2008) 192–202.

[56] Uganda National Tuberculosis and Leprosy Programme (NTLP), *Annual Report 2023/2024* (Ministry of Health, Uganda, 2024), https://health.go.ug/download/ntlp-uganda-annual-report-2023-2024/.

[57] P. Van den Driessche and J. Watmough, Reproduction numbers and sub-threshold endemic equilibria for compartmental models of disease transmission, *Math. Biosci.* **180**(1–2) (2002) 29–48.

[58] R. S. Wallis, Mathematical models of tuberculosis reactivation and relapse, *Front. Microbiol.* **7** (2016) 669.

[59] World Bank, *World Development Indicators: Uganda Demographic Statistics* (World Bank, 2023), https://data.worldbank.org/; https://data360.worldbank.org/en/economy/UGA.

[60] World Health Organization, *Global Hepatitis Report 2024: Action for Access in Low- and Middle-Income Countries* (WHO, Geneva, 2024), https://www.who.int/publications/i/item/9789240091672.

[61] World Health Organization, *Global Tuberculosis Report 2024* (WHO, Geneva, 2024), https://www.who.int/teams/global-programme-on-tuberculosis-and-lung-health/tb-reports.

[62] Z. Zhuang, L. Sun, X. Song, H. Zhu, L. Li, X. Zhou and K. Mi, Trends and challenges of multi-drug resistance in childhood tuberculosis, *Front. Cell. Infect. Microbiol.* **13** (2023) 1183590.

Math. Open 2026.05. Downloaded from www.worldscientific.com
by 196.43.164.50 on 11/12/26. Re-use and distribution is strictly not permitted, except for Open Access articles.